3. Multi-Level Modeling of PEBB-Based Power System

This chapter presents a methodology to model the PEBB-based power system using the modularized concept. Modularized modeling has two folds of meaning. First, the computer models of system building blocks are developed in the same way as those of the PEBB module. The software construction of the distributed power system using the computer models will be the same as the hardware using PEBB modules. Second, hierarchical modeling approaches are used. Each basic system module or complicated controller or subsystem can be packaged together as one block with input and output terminals as well as parameters that can be adjusted by the users. The packaged blocks can be used to build up a large-scale system. This function is facilitated by the hierarchical modeling features in the Saber simulation software. Meanwhile, the descriptive mast-language provided in the software is used to establish customized models. Three models are discussed in this chapter, the discrete model, which treats the power switches as ideal switches, the large signal average model, which models the system characteristics at lower frequency, and the small signal model, which linearizes the average model above the operation point. Those models are used to simulate and analyze the interactions in different frequency ranges, as shown later in this dissertation.

3.1 Discrete Models Based on PEBB Concept

3.1.1 The Discrete Model of the PEBB module and the Modularized System Structures

Conventional discrete models are device-oriented. This modeling approach becomes inefficient and complicated for a large-scale system. In the modularized modeling approach, the first step is to model the power stage based on the basic system building block – the phase leg.

In order to save simulation time in system level simulations, the power semiconductor devices can be modeled as ideal switches with important parameters such as turn-on and turn-off threshold voltage, turn-on and turn-off time, on-resistance/voltage drop, off-resistance, and so on. These parameters can be adjusted in the model. This PEBB module has four terminals: one control terminal, s, and three power terminals: the collector of the top switch, p, the emitter of the bottom switch, n, and the middle point, m. The middle point generally is connected to an inductor and the other two points, and p and n, usually are connected to the dc bus. The control signal s is assigned to be the top switch control signal. The bottom switch control signal is assumed to be complementary to s. When s is high, the top switch will be on; if the current is going out from the middle point, the active switch is on. If the current is going into the middle point, the diode is on. Because the inductor current has to be continuous, either top switch or bottom switch has to be on at any moment of operation. This circuit can be modeled as a two-port network with n as a common port connector as shown in Figure 3.1 (a). The current of the port1 and voltage of port2 are state variables: the inductor current and capacitor voltage. By ignoring the dead-time effect, the relationship between the control and port voltage and current are:

$$Vport1 = \begin{cases} Vdc, & s = 1 \\ 0, & s = 0 \end{cases} \tag{3-1}$$

$$Iport2 = \begin{cases} Iport1, & s = 1 \\ 0, & s = 0 \end{cases} \tag{3-2}$$

A typical three-phase system based on the PEBB concept can be constructed as shown in Figure 3.1 (b). It has four bocks, the input and output filter, the power stage containing three phase-leg modules, and a local controller. The higher level control can command and accept signals from the local controller for the hierarchical system monitor and management. The power stage block accepts either ac or dc power. The power switches are programmed by the controller to follow a certain pattern of switching actions and convert the input power into other forms. The controller block receives sensor signals from the input and output in closed loop operations. The input and output filter smoothes input and output voltage/current.

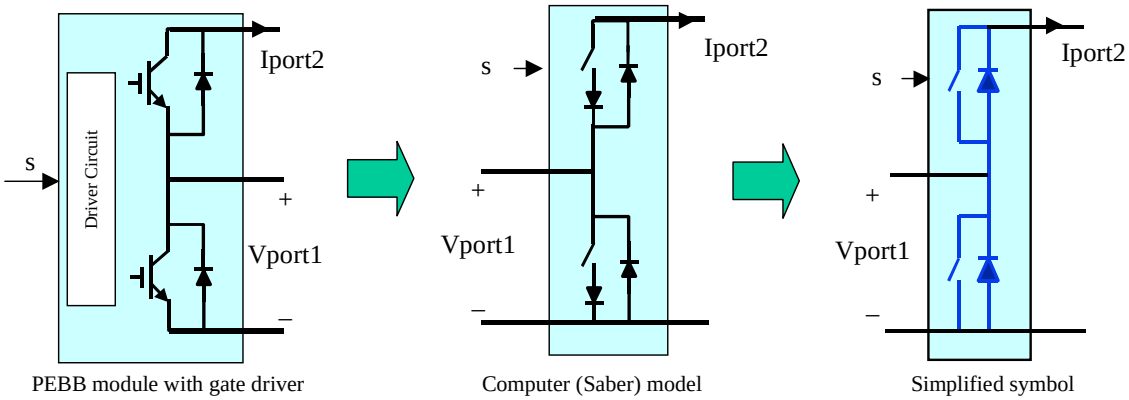

(a)

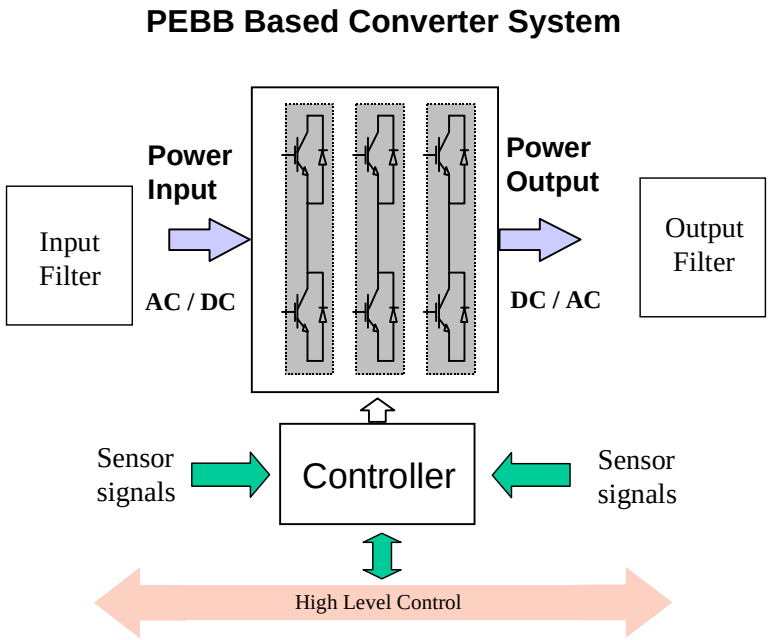

(b)

Figure 3.1 Discrete modeling of PEBB (a) PEBB model, and (b) PEBB-based system structure

3.1.2 The Common Controller Structures for Three-Phase Voltage Source Converters

The controller block generally is implemented in a digital signal processor (DSP) with A/D, D/A converters, programmable logic devices, and so forth. Even though the control algorithm is implemented as software, which depends on the DSP, the common controller structure exists for typical three-phase converters or inverters as shown in Figure 3.2. This is easy to understand, because when a motor drive operates in a generator mode, the inverter becomes a rectifier with its previous controller. The PEBB common controller structure includes four essential parts: (1) the control intelligence interfacing to high level control, which allows the system monitor and programmability, (2) the outer loop, which is a voltage loop for the PWM rectifier and a speed loop for a Permanent Magnet Synchronous Motor (PMSM) motor drive, (3) the inner loop, which has two-channel current loops on dq coordinates for three-phase converters, and (4) the pulse width modulator, which is normally a SVM.

The signal flow path starts with the outer loop. It generates the reference signal for the inner loop – the current loop, which controls the active and reactive power through the two channels, respectively. The output of the current loop controller will be sent to the Space Vector Modulation (SVM) block, which generates the PWM signals for the active devices. Conventional PI or PID controllers can be used directly for the voltage and current loop compensators. Therefore, more attention has been paid to the current loop controller and the SVM.

The following analysis shows the commonality of the current loop controller between the boost PFC rectifier and the Voltage Source Inverter (VSI) fed Permanent Magnet Synchronous Motor (PMSM) drive. The controller is implemented in DQ coordinates. Even though the power conversion modules can be modeled with discrete events, the current loop controllers are established on the average models. As shown in Figure 3.3, two controllers share a common structure. They accept the reference and feedback signals from the outside. The errors are processed through d and q channel compensator Hid and Hiq. There are cross signal flow paths between the two channels, which decouple the coupling terms in the plant transfer function. In order to see the difference in the decoupling terms, the large signal average dq model of the front-end PFC rectifier and VSI fed PMSM motor have to be examined to see how they are coupled. The models are given by equation (3-3) and (3-4) respectively.

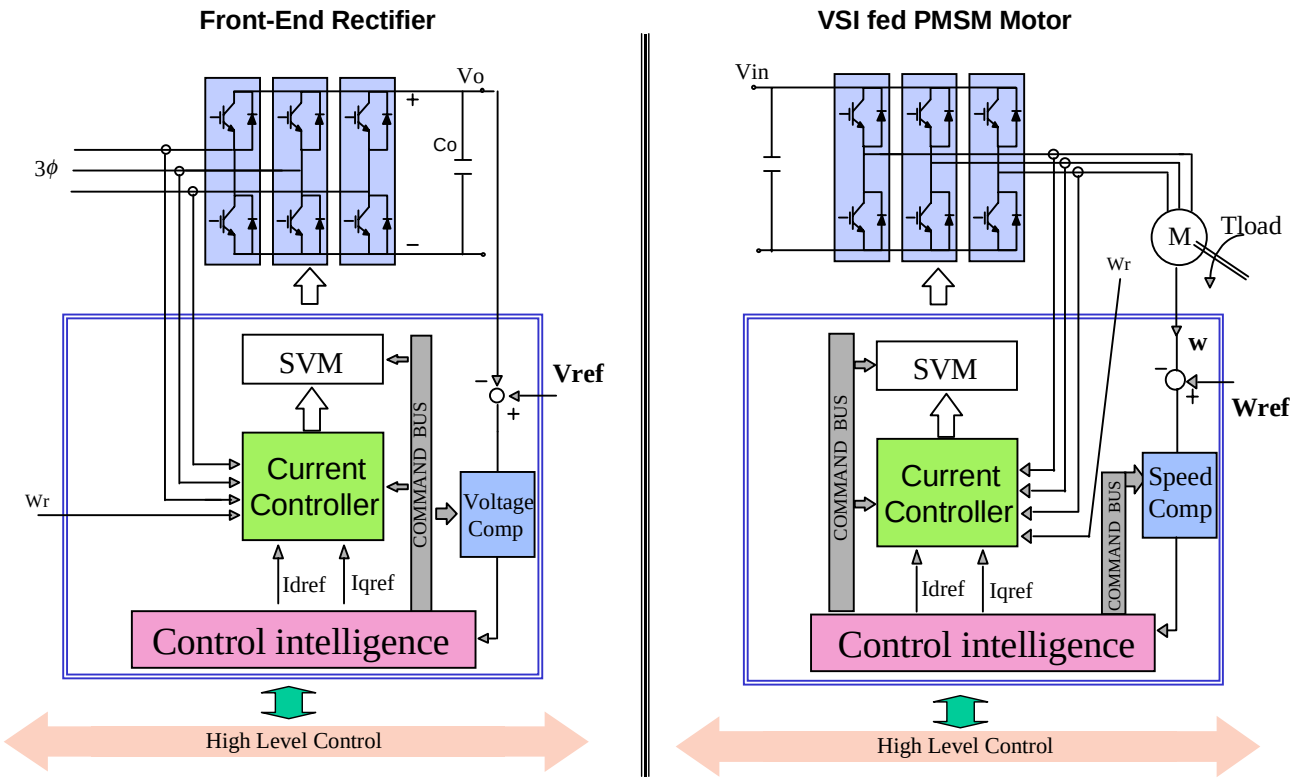

Figure 3.2 The common controller structures for three-phase PEBB system

$$\frac{d}{dt}\begin{bmatrix} i_d \\ i_q \\ v_o \end{bmatrix} = \begin{bmatrix} 0 & 3\omega & -\frac{D_d}{L} \\ -3\omega & 0 & -\frac{D_q}{L} \\ \frac{D_d}{C} & \frac{D_q}{C} & 0 \end{bmatrix}\begin{bmatrix} i_d \\ i_q \\ v_o \end{bmatrix} + \begin{bmatrix} \frac{1}{L} & 0 & 0 \\ 0 & \frac{1}{L} & 0 \\ 0 & 0 & -\frac{1}{C} \end{bmatrix}\begin{bmatrix} v_d \\ v_q \\ i_o \end{bmatrix} \tag{3-3}$$

$$\frac{d}{dt}\begin{bmatrix} i_d \\ i_q \\ \omega \end{bmatrix} = \begin{bmatrix} -\frac{R}{L_d} & (p\frac{L_q}{L_d})\omega & 0 \\ -(p\frac{L_d}{L_q})\omega & -\frac{R}{L_q} & k_t \\ \frac{3}{2J}p(L_d - L_q)I_q & \frac{3}{2J}(k_t + p(L_d - L_q)I_d & -\frac{k_{load}}{J} \end{bmatrix}\begin{bmatrix} i_d \\ i_q \\ \omega \end{bmatrix} + \begin{bmatrix} \frac{1}{L_d} & 0 \\ 0 & \frac{1}{L_q} \\ 0 & 0 \end{bmatrix}\begin{bmatrix} D_d \\ D_q \end{bmatrix}\frac{V_{DC}}{\sqrt{3}} + \begin{bmatrix} 0 \\ 0 \\ \frac{K_{load}}{J} \end{bmatrix}\Omega \tag{3-4}$$

The derivation process is skipped [D10, A8]. In equation (3-3) the parameters for the boost PFC rectifier are defined as follows:

v_d, i_d, D_d: the d channel component: voltage, current, and duty cycle

v_q, i_q, D_q: the q channel component: voltage, current, and duty cycle

v_o, i_o: the output voltage and current

ω: the angular input line frequency

L: the input boost inductor

C: The output dc bus capacitor

In equation (2-4) the parameters for the PMSM are defined as follows:

i_q: q-axis components of the stator voltage and current

i_d: d-axis components of the stator voltage and current

V_{DC}, I_{DC}: the dc bus voltage and current

p: number of pairs of poles

R: stator phase resistance

L_d: stator inductance in d axis

L_q: stator inductance in q axis

K_t: torque constant.

ω: instantaneous rotational speed

Ω: rotational speed at the point where the load torque slope changes

J: moment of inertia

It can be seen that the d and q channels are coupled in equation (3-3) and (3-4). The d channel current is affected by the q channel current, and vice visa. The coupled terms can only be decoupled by the control variable: Dd and Dq. These are proportional to the output of the current loop controller Vcd and Vcq. Therefore, extra terms are added into Vcd and Vcq after the compensator Hid and Hiq. Taking the d channel of the rectifier as an example, in order to remove the term $3\omega Li_q$ as shown in equation (3-5), the decoupling duty cycle Dd′ has to be added as shown in (3-6)

$$3\omega LI_q - D_d' v_o = 0 \tag{3-5}$$

$$D_d' = \frac{3\omega LI_q}{v_o} \tag{3-6}$$

Figure 3.3 shows the equations of the decoupling terms for PFC and VSI fed PMSM, which are nonlinear functions of the rotation frequency ω and the dq channel current I_d and I_q. In these equations, because the bandwidth of the current loop, the inner loop, is much higher than the outer loop, the dc bus voltage is assumed to be a constant.

3.1.3 Discrete Model of Space Vector Modulation Using Saber

In a three-phase system, because each phase is connected to either the positive or negative dc rail, there are a total of 2^3 switching topological states. Each state is defined as a space vector expressed by three letters composed of p and n. For example, the pnn vector means that phase A is connected to the positive dc rail, and phases B and C are connected to the negative dc rail. The ppp and nnn vectors are called the zero vectors. The rest of them are called the active vectors [D8, D16]. The six active vectors are distributed evenly in a hexagon as shown in Figure 3.4. The two zero-vectors can be viewed as being perpendicular to the hexagon plane. The hexagon is divided into six sectors by the six vectors on the plane. Each sector can be divided again as small sectors by the dashed lines as shown in Figure 3.4. Inside the hexagon, the reference vector rotates with the modulation frequency. Its length is determined by the modulation index. SVM is a process of combining the space vectors to synthesize the reference vector. The projections of the reference vector onto the adjacent vectors are defined as d1 and d2. The calculation of d1 and d2 in different sectors are given in Table 3.1

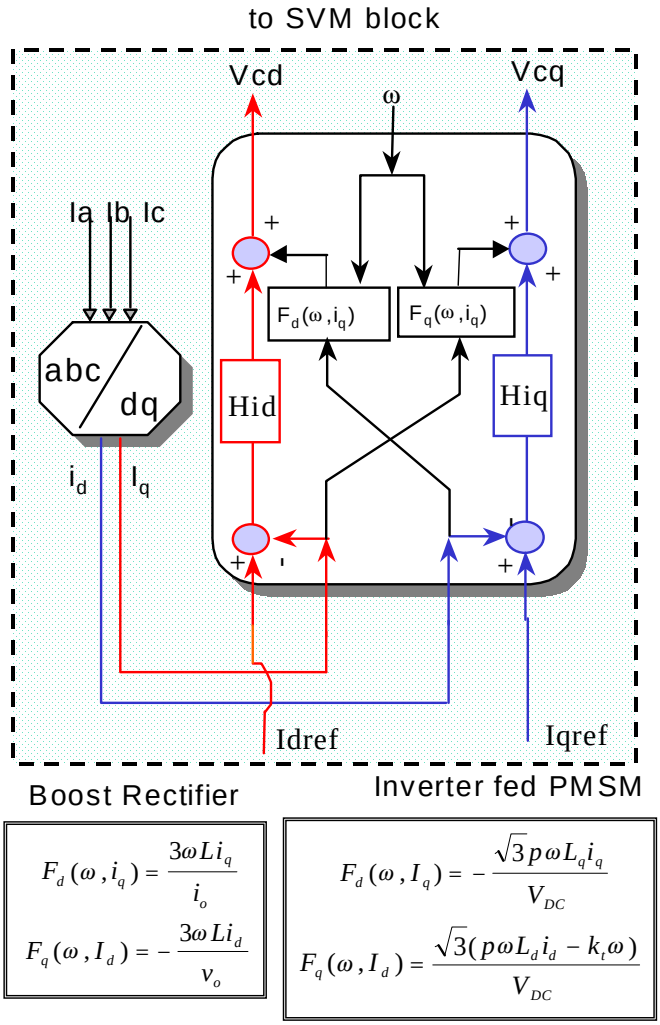

Figure 3.3 Common current loop controller structure for boost PFC rectifier and VSI-fed PMSM

Table 3.1 Calculation of d1 and d2 in different sectors

Sectors	I, IV	II(r*),V(l*)	III, VI	II(l*), V(r*)
d1	$\lvert d_\alpha \rvert - \frac{\lvert d_\beta \rvert}{\sqrt{3}}$	$\lvert d_\alpha \rvert + \frac{\lvert d_\beta \rvert}{\sqrt{3}}$	$2\frac{\lvert d_\beta \rvert}{\sqrt{3}}$	$\frac{\lvert d_\beta \rvert}{\sqrt{3}} - \lvert d_\alpha \rvert$
d2	$2\frac{\lvert d_\beta \rvert}{\sqrt{3}}$	$\frac{\lvert d_\beta \rvert}{\sqrt{3}} - \lvert d_\alpha \rvert$	$\lvert d_\alpha \rvert - \frac{\lvert d_\beta \rvert}{\sqrt{3}}$	$\lvert d_\alpha \rvert + \frac{\lvert d_\beta \rvert}{\sqrt{3}}$

* l: left half sector; r: right half sector

In Table 2.1, d_α and d_β are the output of current loop controller mapped onto the stationary coordinate by (3-7), where dd and dq equal to the output of current loop controller: Vcd and Vcq.

$$\begin{bmatrix} d_\alpha \\ d_\beta \end{bmatrix} = \begin{bmatrix} \cos(\omega t) & -\sin(\omega t) \\ \sin(\omega t) & \cos(\omega t) \end{bmatrix} \begin{bmatrix} d_d \\ d_q \end{bmatrix} \quad (3\text{-}7)$$

The d0 can be calculated from d1 and d2 by:

$$d0 = 1 - d1 - d2 \quad (3\text{-}8)$$

If the switching cycle is defined as Ts, the duration of d1, d2, and d0 can be obtained by:

$$T1 = d1Ts \quad (3\text{-}9a)$$

$$T2 = d2Ts \quad (3\text{-}9b)$$

$$T0 = d3Ts \quad (3\text{-}9c)$$

The correlation between T1, T2, T0 and the SVM output is shown in Figure 3.4 (b), where the 60-degree clamped SVM is used as the example.

3.1.4 Simulation Waveforms Using the Discrete Model

Figure 3.5 illustrates a series of simulation waveforms using the discrete model. Figure 3.5 (a) shows the waveforms of the input voltage and current of a three-phase PFC rectifier; 3.5 (b) and (c) show the typical line-to-line voltage and the dc link input current waveform of the three-phase inverter, respectively. As shown in these waveforms, the voltage and current waveforms have discrete switching frequency ripples. Discrete models are good for time domain simulation, but the calculations take a very long time, especially for low modulation and high switching frequencies. For example, a 60 Hz line frequency and 20 kHz switching frequency system would take over six thousand iterations in one switching cycle with step size of one twentieth of a switching period.

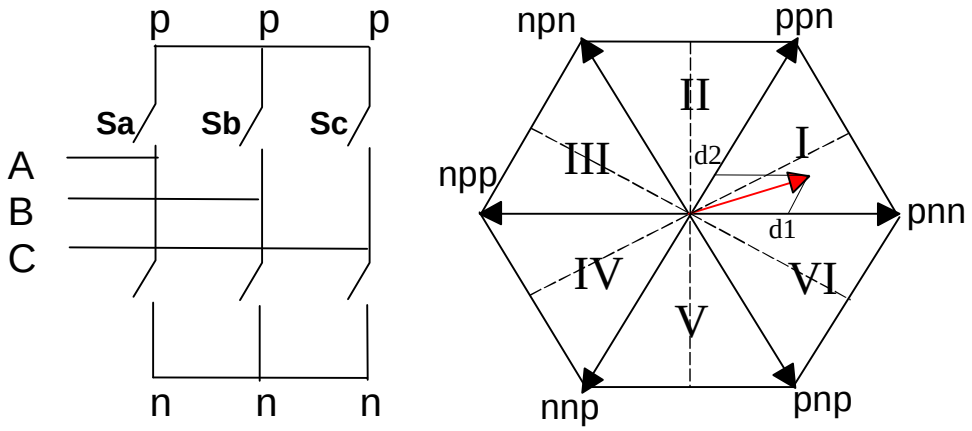

(a)

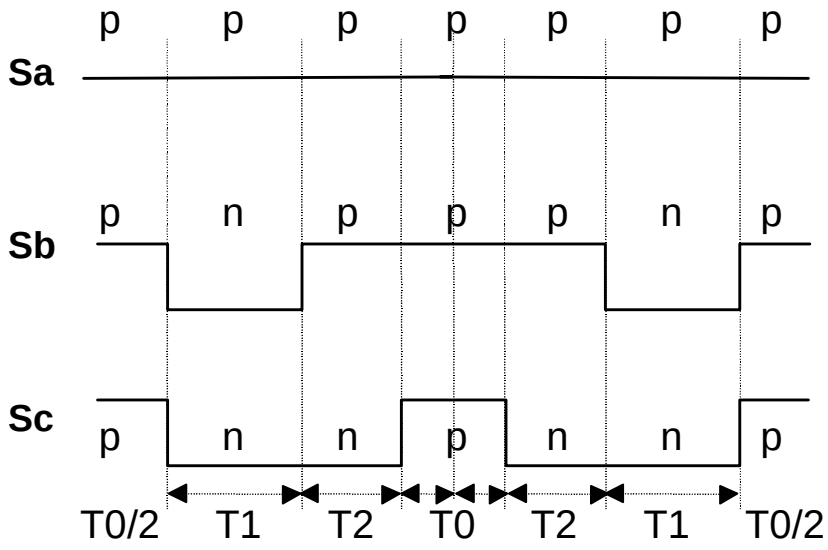

(b)

Figure 3.4 Space vector Modulation, (a) Space vectors and sector definition, (b) The output of the SVM defined by T1,T2, and T0

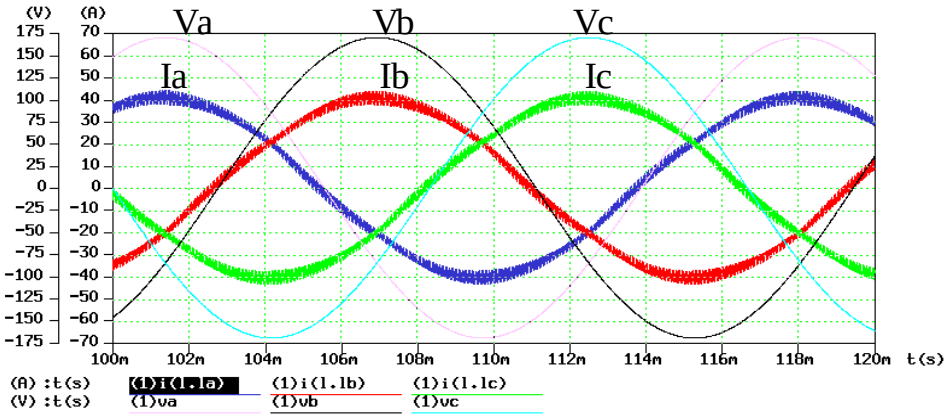

(a)

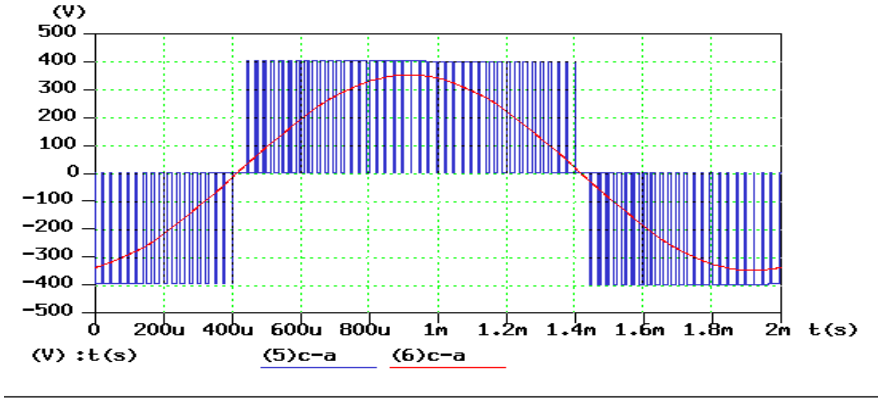

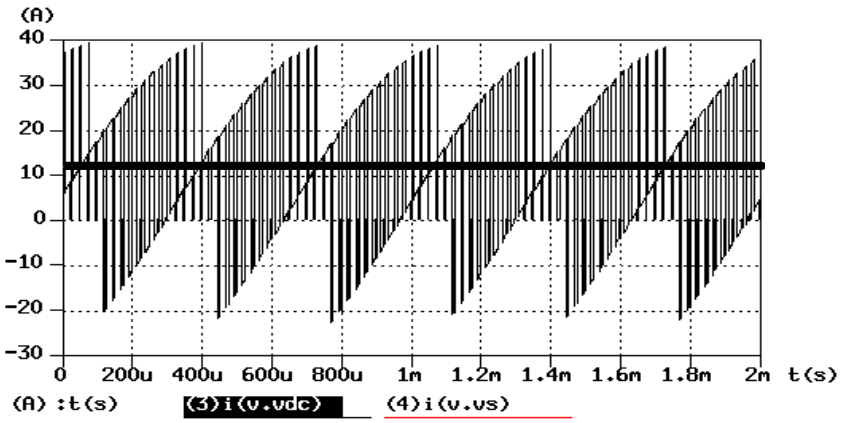

(b) (c)

Figure 3.5 Simulation waveforms using discrete model, (a) three-phase rectifier input voltage and current, (b) and (c) VSI line-to-line voltage and the dc link input current

3.2 The Average Large Signal Model

The conventional average large signal model of the three-phase system is developed on the dq coordinates. This section presents a new approach of developing the large signal average circuit model based on the PEBB concept.

3.2.1 Modeling of the PEBB Module

In the following analysis, the three-phase PWM rectifier is taken as the example.

In the discrete model, the control variable of the phase-leg module is s. The duty cycle of the phase leg can be obtained by averaging s over a switching cycle.

$$Di = \langle s \rangle \tag{3-10}$$

Assume that all the active switches and diodes are ideal, i.e., that there is no on-voltage drop in conduction and that the device blocking impedance is infinity. The averaged port voltage and current can be expressed by (3-11):

$$\begin{aligned} \langle V_{port1} \rangle &= D_i V_{port2} \\ \langle I_{port2} \rangle &= D_i I_{port1} \end{aligned} \tag{3-11}$$

Therefore, the PEBB phase-leg can be considered as a black box with two ports and a control variable – the duty cycle. The input voltage of port 1 and the output current of port 2 are controlled voltage and current source, which is shown in Figure 3.6.

3.2.2 Modeling of Multi-Phase System Based on Phase Legs

With the averaged phase leg model, multi-phase converters composed of PEBB modules can be modeled by simply replacing the phase-leg with the two-port network, as illustrated in Figure 3.7 as a three-phase system. The objective of the three-phase rectifier is to generate a sinusoidal current at the middle-point-connected inductors. The most conventional way to produce such a sinusoidal current in the inductor is to use a sinusoidal control signal D_i in the average sense. In this case, the analysis of the averaged three-phase system can be simplified to single phase, because the averaged voltage potential of the negative dc rail is the same as the neutral point of the source.

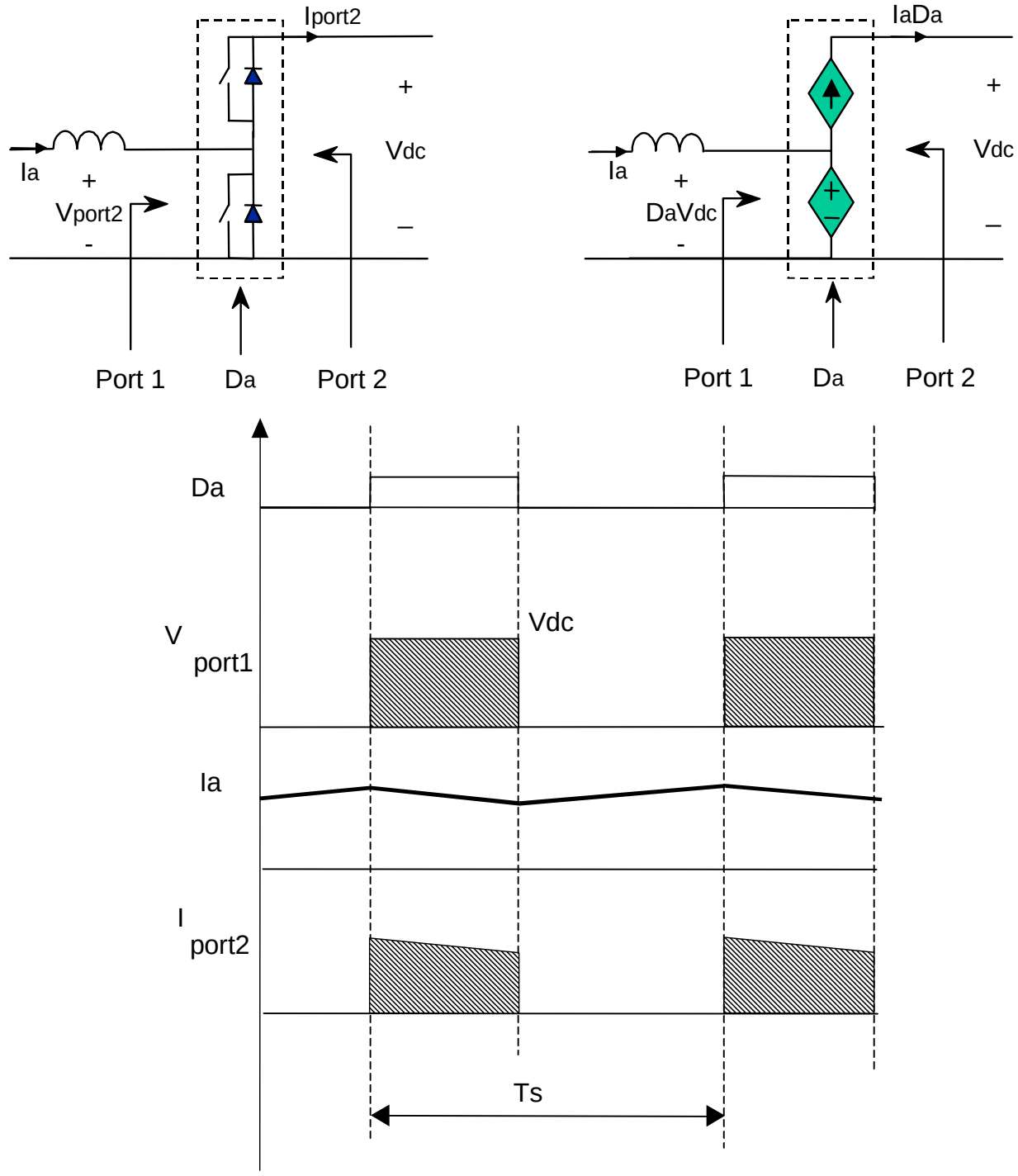

Figure 3.6 Derivation of the phase-leg PEBB model

It has been found that in three converters, certain advantages can be achieved, such as reduced commutation times and switching loss and/or better THD, by injecting a common mode voltage onto the modulation signals. The common mode voltage can be a third order sinusoidal, a triangle, or other waveform. Space vector modulation schemes have different common mode voltages when zero vectors are used differently. The common mode voltage is also a function of modulation index, the lower the modulation index, the higher the common mode voltage. In many situations, the common mode voltages are discontinuous. But in any case, because Di is a periodic signal, it can be written as a Fourier Series containing the fundamental modulation frequency and other frequencies.

$$D_i = D_{i\omega} + \sum_{n=0,n\neq 1}^{n=\infty} D_{in\omega} \tag{3-12}$$

Therefore, the modulated voltage applied to phase a at the port 1 is:

$$V_a = D_a V_{port2} = (D_{a\omega} + \sum_{n=0,n\neq 1}^{n=\infty} D_{an\omega}) V_{port2} = D_{a\omega} V_{port2} + D_{common} V_{port2} \tag{3-13}$$

It has a modulation frequency component and common component. The expression for the other phases can be obtained also.

$$V_b = D_b V_{port2} = D_{b\omega} V_{port2} + D_{common} V_{port2} \tag{3-14}$$

$$V_c = D_c V_{port2} = D_{c\omega} V_{port2} + D_{common} V_{port2} \tag{3-15}$$

At the output side, the total current output current at port two are:

$$I_{out} = D_a I_a + D_b I_b + D_c I_c = D_{a\omega} I_a + D_{b\omega} I_b + D_{c\omega} I_c + D_{common}(I_a + I_b + I_c) \tag{3-16}$$

Equation (3-14) to (3-16) show that the common mode voltage does not contribute to the three-phase input and the dc bus output current. The large-signal DQ model was derived by ignoring such a component [D15]. Based on the phase leg model, the averaged three-phase converter the can be obtained:

$$\frac{d}{dt}\begin{bmatrix} i_a \\ i_b \\ i_c \end{bmatrix} = -\frac{R_L}{L}\begin{bmatrix} i_a \\ i_b \\ i_c \end{bmatrix} + \frac{1}{3L}\begin{bmatrix} 2 & -1 & -1 \\ -1 & -1 & -1 \\ -1 & -1 & 2 \end{bmatrix}\begin{bmatrix} v_a \\ v_b \\ v_c \end{bmatrix} - \frac{v_{dc}}{3L}\begin{bmatrix} 2 & -1 & -1 \\ -1 & -1 & -1 \\ -1 & -1 & 2 \end{bmatrix}\begin{bmatrix} d_a \\ d_b \\ d_c \end{bmatrix} \tag{3-17a}$$

$$\frac{dv_{dc}}{dt} = \frac{R_{load}}{C(R_{load} + R_c)}\begin{bmatrix} i_a & i_b & i_c \end{bmatrix}\begin{bmatrix} d_a \\ d_b \\ d_c \end{bmatrix} - \frac{v_{dc}}{C(R_{load} + R_c)} \tag{3-17b}$$

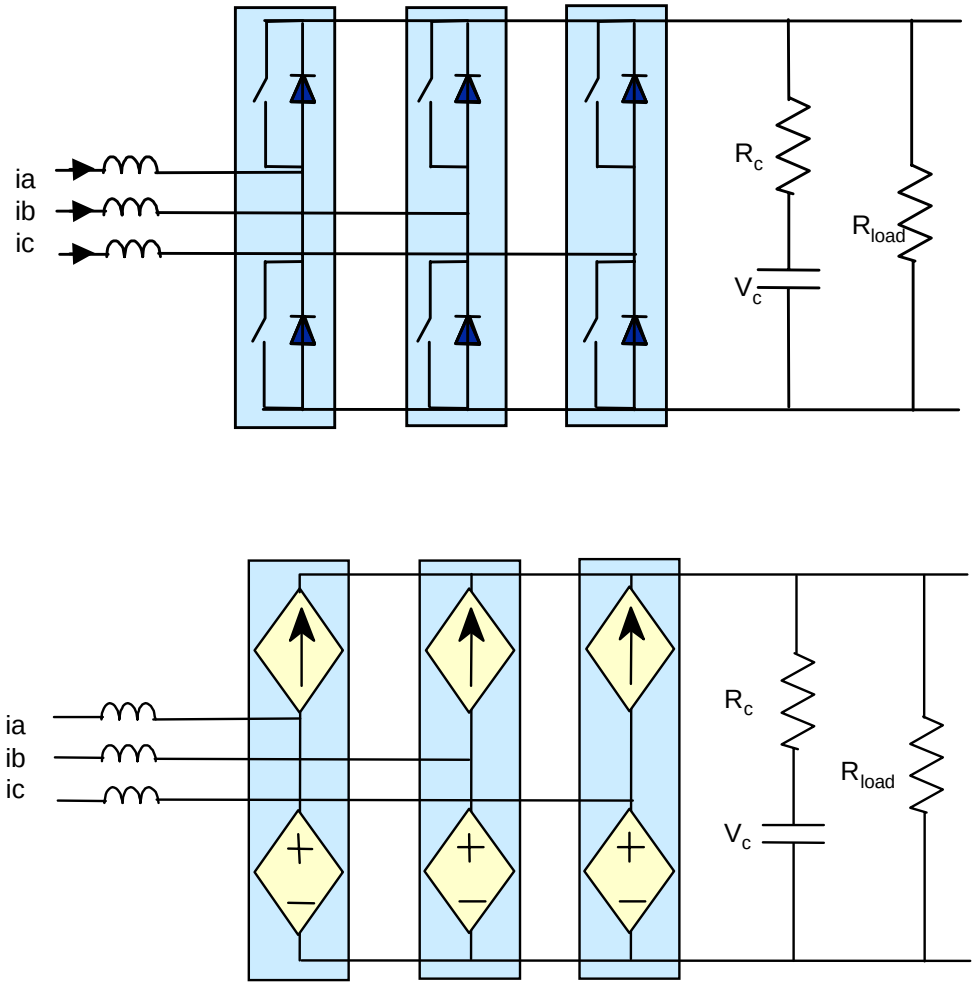

Figure 3.7 The equivalent circuit model of the three-phase PWM rectifier

where Vdc is the dc bus voltage, R_{load} is the load resistance, R_L and R_c are the parasitic resistance of the inductor and the capacitor. The common mode component is included in the model, but it is not contribute to three-phase input and output current.

3.2.3 Modeling of Space Vector Modulation

3.2.3.1 The Principle of SVM Average Model

Assume that the SVM is a black box. The inputs to this box are the modulation index from the *dq* (or alpha-beta) channel controllers and the switching clock. The outputs of this box are the control signals for active switching devices. The SVM calculation is essentially a process of mapping variables from the *dq* coordinate to the stationary coordinate through the space vectors. This process keeps the synthesized space vector rotating as a circle, while leaving the zero-axis free. As a consequence, it guarantees that the modulated line-to-line voltage will always be sinusoidal. It realizes a higher line-to-line voltage with a given bus by actually injecting a common mode signal into the phases.

By applying the average concept to the output of the SVM, a cycle-by-cycle average model of the SVM is obtained. In this model, instead of providing the gate signal as a pulse in each switching cycle, the SVM generates the duty ratio in terms of *da*, *db*, and *dc*, which are numeric values comprised of small pieces of duty-ratios calculated in each simulation step. Different from the conventional average model, the averaged SVM model calculates the duty cycles at least one time in each switching cycle at the beginning of the switching clock. Because of this, it can capture the discontinuity of the averaged PWM signal. Figure 3.8 illustrates the principle of the duty cycle calculation in three switching cycles. Sa, Sb, and Sc are the discrete control signal for the top active switches of the three phase legs. Da, Db, and Dc are calculated according to d1,d2 and d0. The relationship between the phase duty cycle and d1, d2, and d0 in 60-degree clamping SVM are shown in Table 3.2. The d1,d2 and d0 are mapped from d_α and d_β from table 3.1. The definitions of the sectors are shown in Figure 3.9. Da, Db, and Dc are composed of fundamental components and a common-mode component as shown in equation (3-18) and (3-19).

$$\begin{bmatrix} da \\ db \\ dc \end{bmatrix} = \begin{bmatrix} d_{a\omega} \\ d_{b\omega} \\ d_{c\omega} \end{bmatrix} + \begin{bmatrix} d_0 \\ d_0 \\ d_0 \end{bmatrix} \tag{3-18}$$

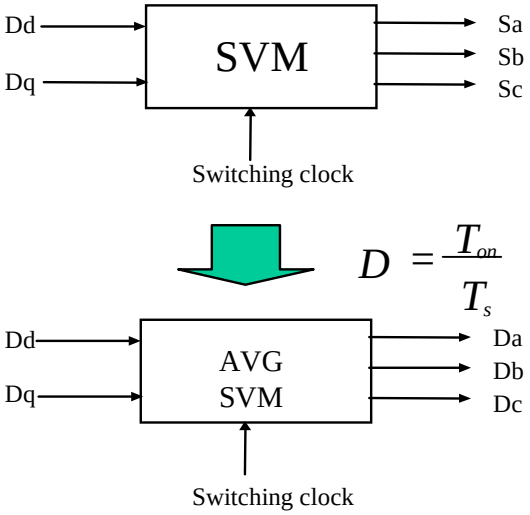

$$0 \leq D_i \leq 1 \qquad i = a, b, c$$

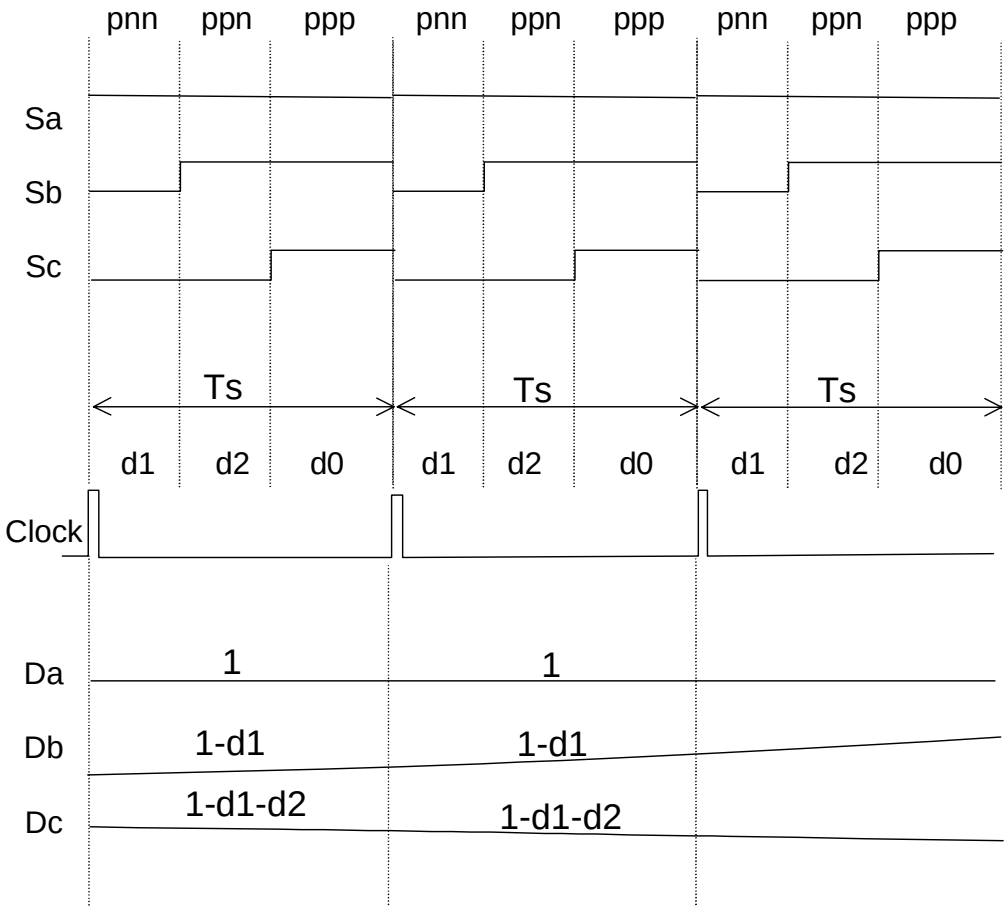

Figure 3.8 An average model of SVM

$$\begin{bmatrix} d_{a\omega} \\ d_{b\omega} \\ d_{c\omega} \end{bmatrix} = \frac{2}{3}\begin{bmatrix} 1 & 0 \\ -\frac{1}{2} & \frac{\sqrt{3}}{2} \\ -\frac{1}{2} & -\frac{\sqrt{3}}{2} \end{bmatrix}\begin{bmatrix} d_\alpha \\ d_\beta \end{bmatrix} = \frac{2}{3}\begin{bmatrix} \cos(\omega t) & -\sin(\omega t) \\ \cos(\omega t - \frac{2\pi}{3}) & -\sin(\omega t - \frac{2\pi}{3}) \\ \cos(\omega t + \frac{2\pi}{3}) & -\sin(\omega t + \frac{2\pi}{3}) \end{bmatrix}\begin{bmatrix} v_d \\ v_q \end{bmatrix} \quad (3\text{-}19)$$

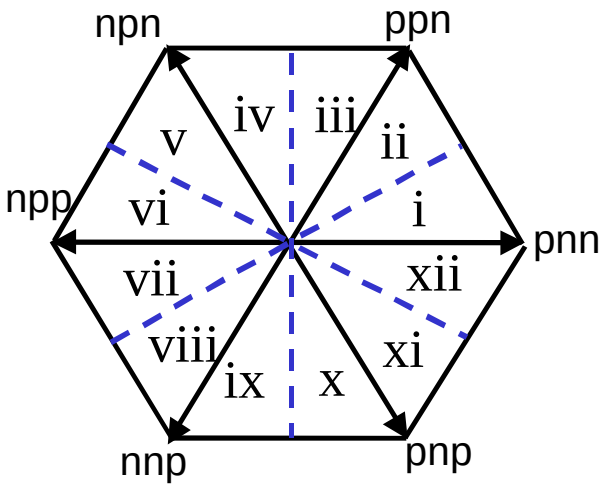

Figure 3.9 Definitions of the sectors in the hexagon

Table 3.2 Mapping between da, db, dc, d0 and d1,d2 in 60-degree clamping SVM

Sector	i	ii	iii	iv	v	vi	vii	viii	ix	x	xi	xii
da	1	d1+d2	d1	1-d2	1-d1-d2	0	0	1-d1-d2	1-d1	d2	d1+d2	1
db	1-d1	d2	d1+d2	1	1	d1+d2	d1	1-d2	1-d1-d2	0	0	1-d1-d2
dc	1-d1-d2	0	0	1-d1-d2	1-d1	d2	d1+d2	1	1	d1+d2	d1	1-d2
d0	$\frac{3-2d_\alpha}{3}$	$\frac{d_\alpha+\sqrt{3}d_\beta}{3}$		$\frac{3+d_\alpha-\sqrt{3}d_\beta}{3}$		$-\frac{2}{3}d_\alpha$		$\frac{3+d_\alpha+\sqrt{3}d_\beta}{3}$		$\frac{d_\alpha-\sqrt{3}d_\beta}{3}$		$\frac{3-2d_\alpha}{3}$

3.2.3.2 Implementation with Saber Template

The distinctive feature of the average SVM model is the mixed digital and analog calculation implemented with Saber mast language. The template has six parts, the template header, global variable declaration, local variable declaration, template body, and output. The global and local variable declaration defines the variables used in the calculation. The template body consists of a digital and an analog part. The digital part calculates the sector information according to the rotating dq parameter triggered by each switching clock. The analog part calculates the duty cycles depending on which sector the reference is in. Figure 3.10 shows two examples of SVMs using the discrete model and the average model. As shown in this Figure, the shapes of the averaged SVM are different because the zero vectors are used differently. The 60-degree clamping SVM has a jump every 60-degrees. Figure 3.11 further illustrates that the jumps can be captured at exactly the beginning point of the switching clock. This is because the position of the rotating reference vector is calculated according to the switching clocks. This feature allows the averaged SVM to maintain the exact common mode signal in the duty cycles.

3.2.4 Systems Constructed from Average Phase Leg and SVM Models

The circuit model based on the average phase-leg and SVM model keeps all the features of the real circuit as shown in Figure 3.12 (a). In comparison, the dq average model is shown in Figure 3.12 (b).

The first model shows the same system structure as that of the real circuit. It has two control loops: the inner current loop and the outer voltage loop. The voltage loop senses the output voltage and compares it with a given reference. The error signal is given to a voltage loop compensator. The output of the voltage loop controller provides the reference for the d channel current loop, which is related to the active power of the system. The q channel, which is related to the reactive power, is given a reference of zero in order to achieve a power factor correction operation. The current loop references are compared with the feedback signal, id and iq, which are transformed from the abc coordinate. The current loop controller generates the duty cycle in the d and q channels. These duty cycles are mapped into the abc coordinate in SVM. The output of SVM, da, db, and dc are sent to the power stage as the control sources for the controlled voltage and current source.

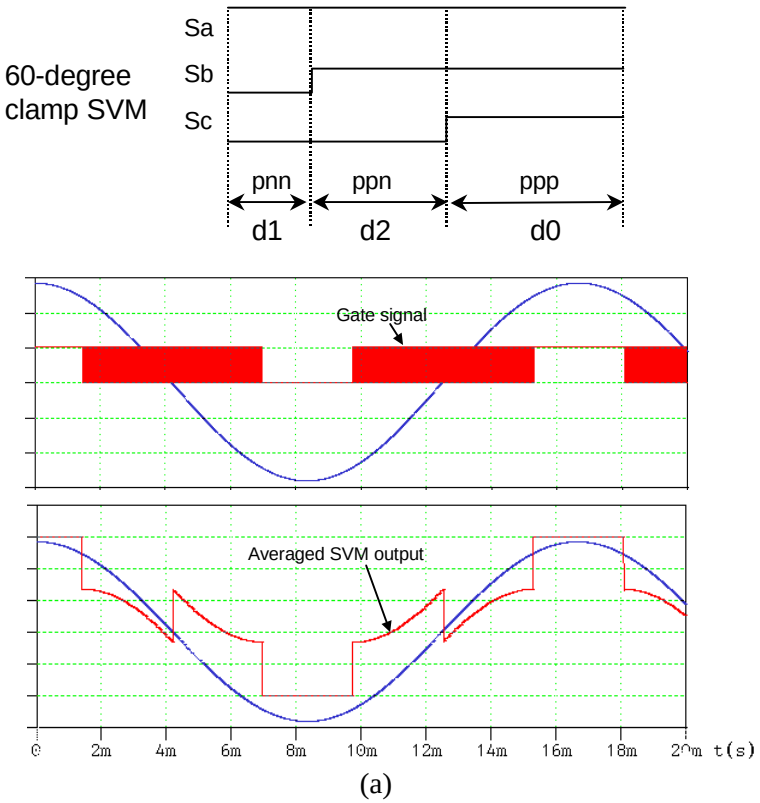

(a)

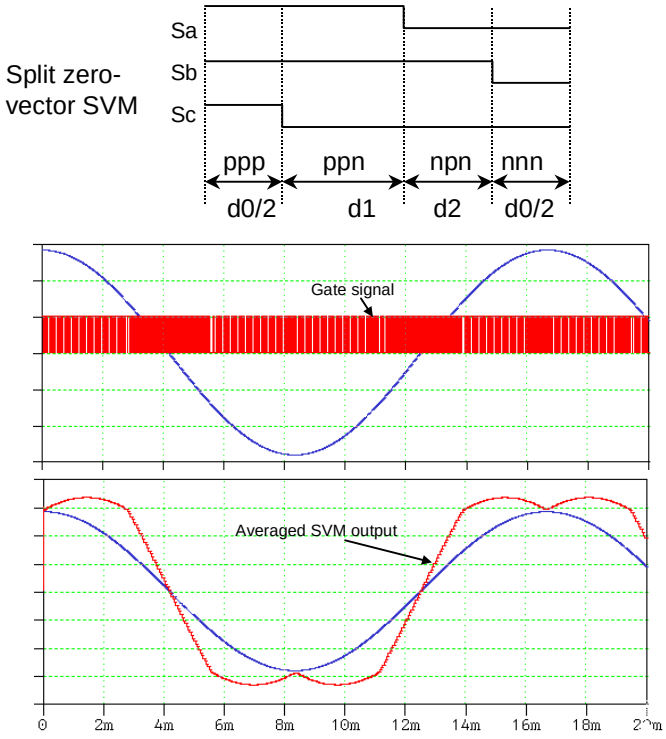

Figure 3.10 The output of averaged SVM with different schemes

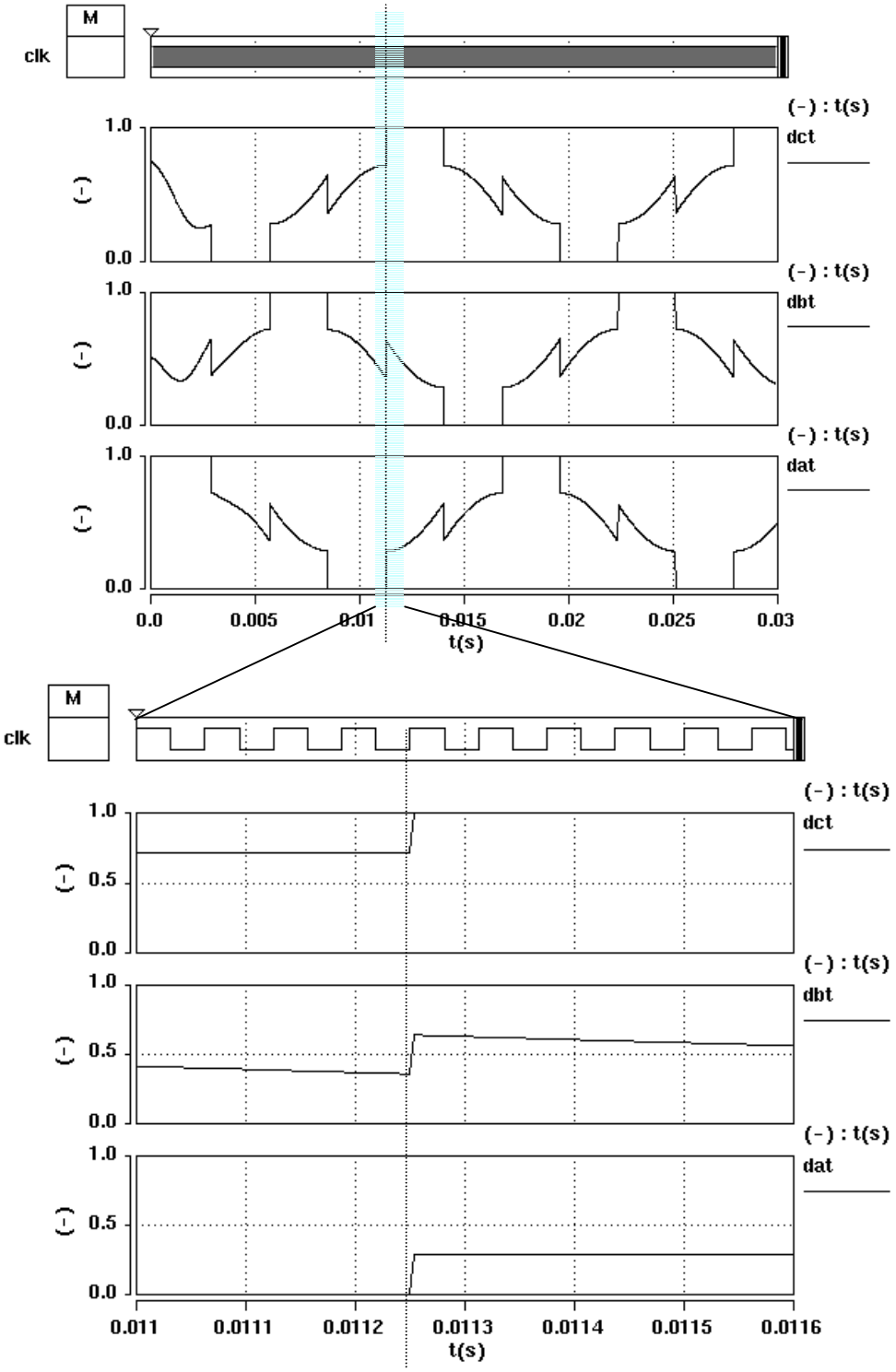

Figure 3.11 The discontinuity captured by the averaged SVM

On the other hand, in the dq model, the three-phase voltage is transformed into dq coordinates first. The power stage is connected to Vd and Vq. The calculation of id, and iq depends on the values of dd, dq, Vo and the cross coupling terms between the two channels. The control loop structure of the system is almost the same, except that the SVM is modeled as a gain block because da, db, and dc are not needed in the power stage model. The output of the controller, dd and dq, are the control sources in the power stage model. The id and iq are used directly as the feedback signals for the current loop. Meanwhile, id and iq are transformed into ia, ib, and ic again in order to see the loading effect of the rectifier to the three-phase source.

In comparison with the first model, the dq model has to perform abc/dq and dq/abc transformations back and forth in order to get the real circuit information. Secondly, the dq model loses the common mode component information that existed in the real circuit, which is very important in system level analysis. As shown later in this section, for example, if the system ground is defined at the neutral point of the three-phase voltage source, the dc bus will be floated with regard to the ground. But the dq model cannot reflect this information.

3.2.5 Time Domain Simulation

3.2.5.1 Comparison with Discrete Model

With the average PEBB module and SVM model, the system set-up can be established easily. Figure 3.13 shows a three-phase inverter system with open loop operation. The phase legs and SVM in the discrete model simply are replaced by their averaged counterparts. The simulation waveforms match each other very well. The SVM with 60-degree clamping is used in the simulation. As shown in this Figure, the common mode voltage information can be seen in the voltage waveform between the neutral point to the negative dc rail. There would be no such information if the dq model were used.

Similarly, the simulation was performed on a PWM rectifier case. The comparisons of the three-phase input current between the discrete model and the average model are shown in Figure 3.14.

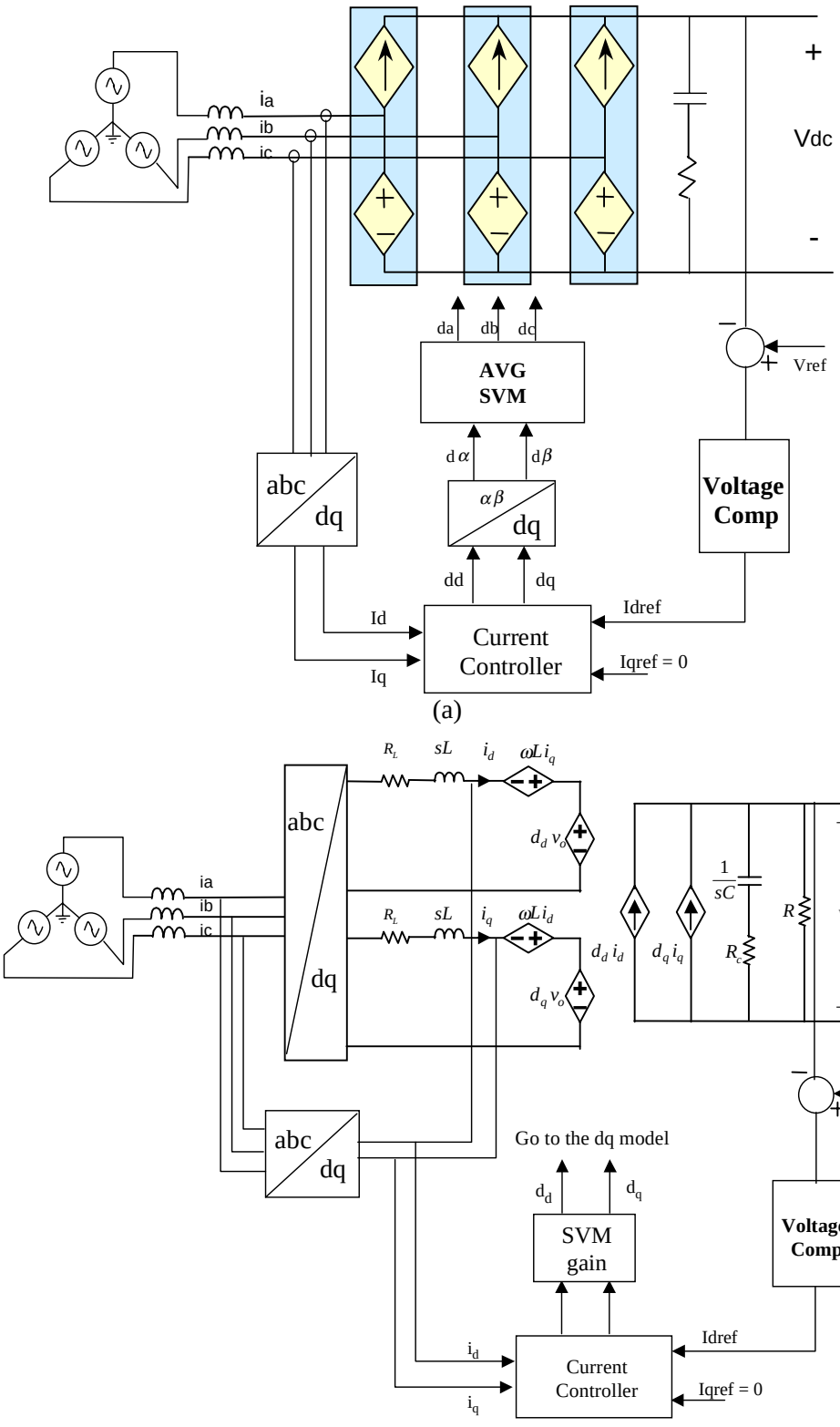

Figure 3.12 The large signal average models of a three-phase rectifier system

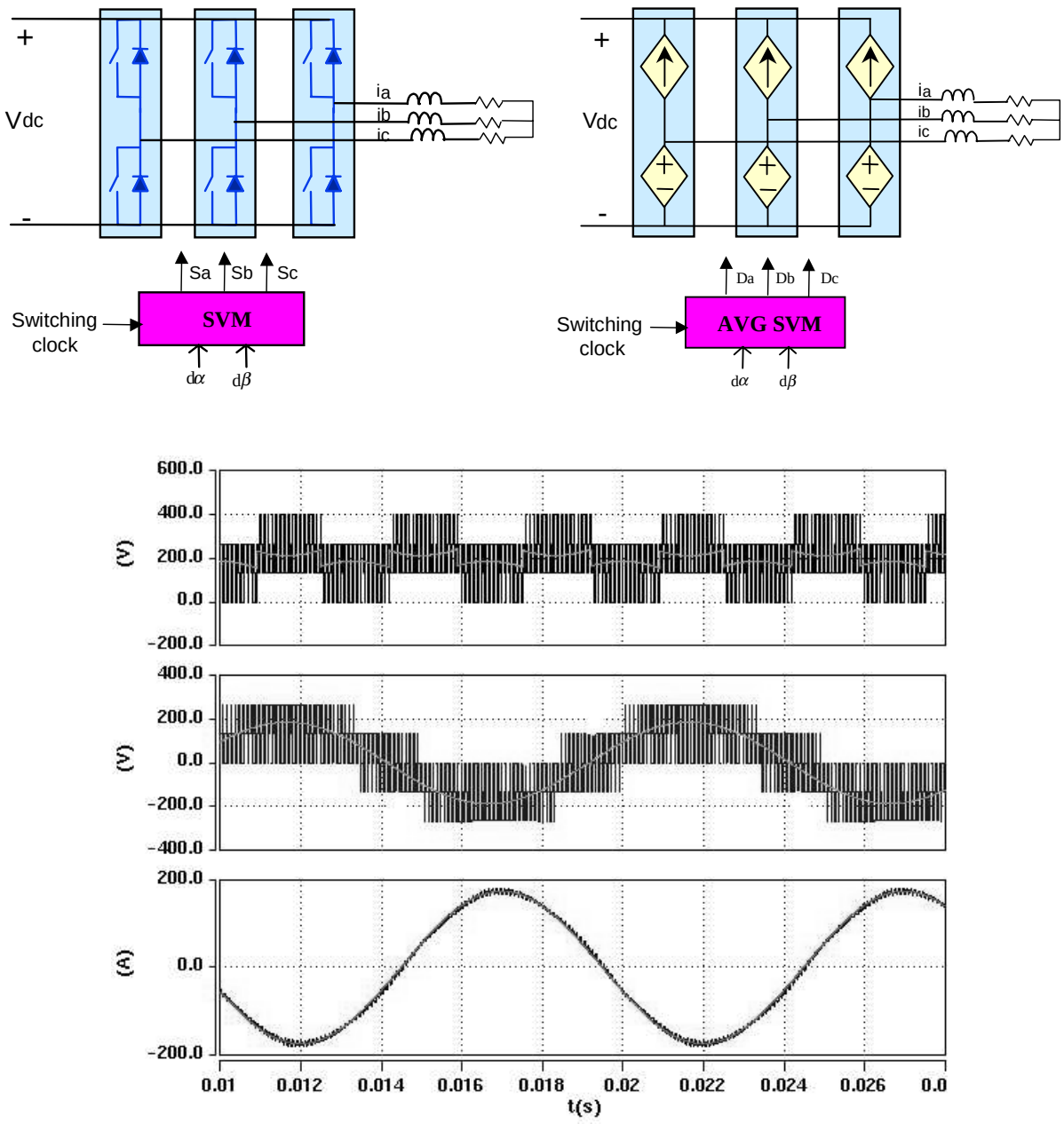

Figure 3.13 Time domain simulation waveform of three-phase inverter with PWM and average model

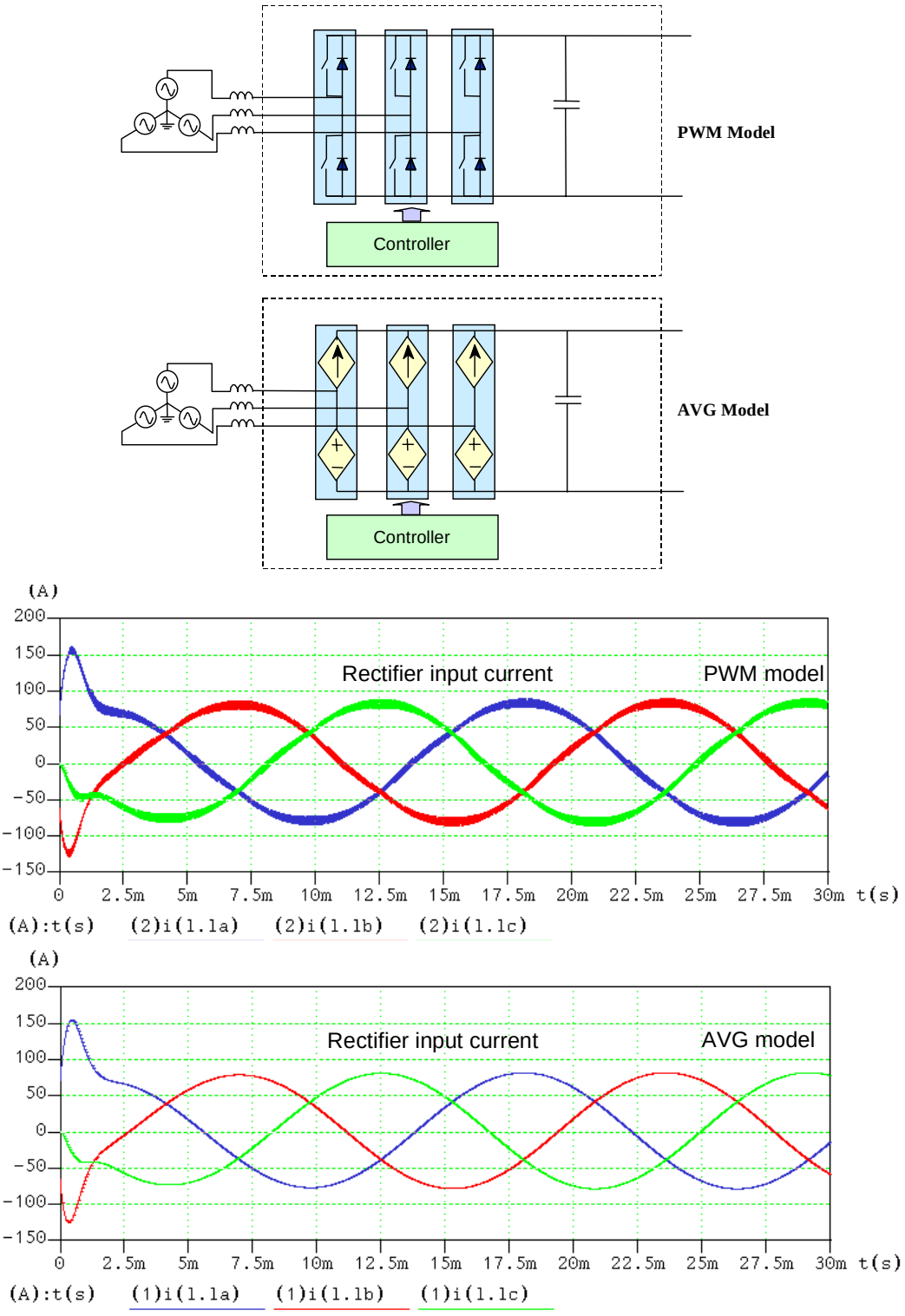

Figure 3.14 Time domain simulation waveforms of PWM rectifier with discrete and averaged model

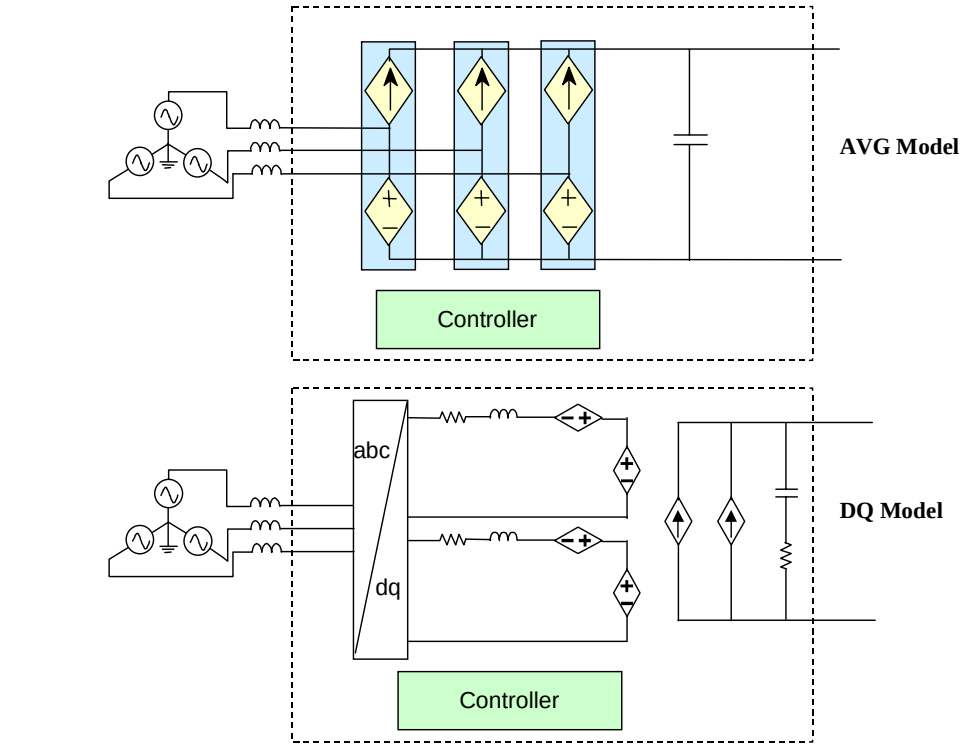

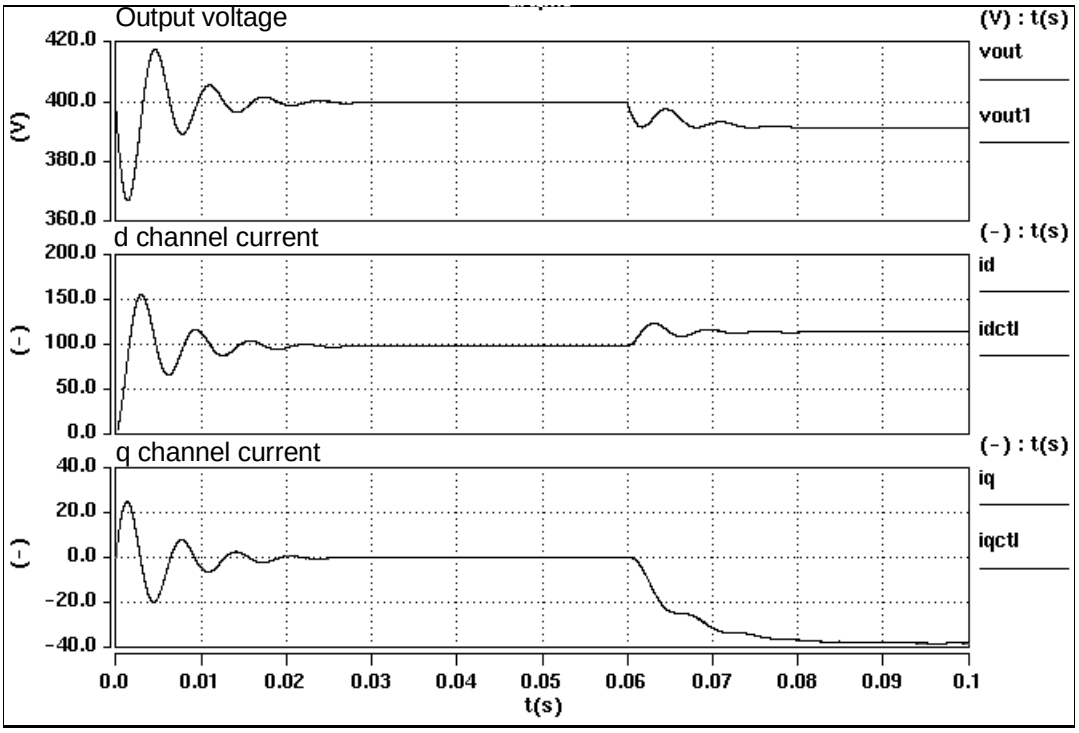

Figure 3.15 The simulation waveform obtained from the averaged abc and dq model (overlapped)

3.2.5.2 Comparison with Average DQ Model

Figure 3.15 shows the open loop systems of the large signal average model and the dq model. The Vcd and Vcq signals are applied to a SVM block. The output of the SVM, Da, Db, and Dc are given to the abc model, and the Dd and Dq transformed from Da, Db, and Dc are used for the dq model. A load step change is applied at 60 ms. As shown in the simulation waveforms, where vout, id, and iq are the variables in the abc circuit model, and where vout1, idctl, and iqctl are obtained from the dq model, all traces are overlapped. The system dynamics are almost the same. There is only a slight difference in the magnitude, which cannot be perceived in this picture.

3.3 Small Signal Analysis Using the Average Model

Conventionally, the small signal analysis of the three-phase system is based on the dq model. The derivation process of the transfer functions with the dq model is complex. For a very large-scale power electronics system with many three-phase converters/inverters, such a process becomes more complicated. In such a case, the easy way is to establish a large signal average model for each subsystem, and then connect these models together to construct a big system. With the large signal average model, the small signal analysis can be performed around an operation point.

If the system is modeled on dq coordinates, the system operation point can be well established in steady state because the dq channel components of the power stage and the control circuit are time invariant. In the average phase-leg model, however, the three-phase voltage, current, and duty cycles are time varying. The conventional operation point concept will not be valid.

3.3.1 Small Signal Perturbation Modulation Effect Caused by SVM

Assume a three-phase system with a SVM control has an operation point as follows:

$$\begin{cases} D_a = D_m \cos(\omega t + \theta) + d_0 \\ D_b = D_m \cos(\omega t - \frac{2\pi}{3} + \theta) + d_0 \\ D_c = D_m \cos(\omega t + \frac{2\pi}{3} + \theta) + d_0 \end{cases} \qquad (3\text{-}20)$$

$$\begin{cases} D_d = D_{d0} \\ D_q = D_{q0} \end{cases}$$

When a perturbation: $\hat{d}_d = d_m \cos(\omega_p t)$ is applied to d channel duty cycle, it becomes:

$$d_d = D_d + \hat{d}_d = D_{d0} + d_m \cos(\omega_p t) \qquad (3\text{-}21)$$

The q channel duty cycle remains the same:

$$d_q = D_{q0} \qquad (3\text{-}22)$$

The zero-sequence component is ignored because it does not contribute the three-phase current. From equation (3-19), the duty cycles on the ABC coordinates can be written as:

$$\begin{bmatrix} d_{a\omega} \\ d_{b\omega} \\ d_{c\omega} \end{bmatrix} = \frac{2}{3} \begin{bmatrix} \cos(\omega t) & -\sin(\omega t) \\ \cos(\omega t - \frac{2\pi}{3}) & -\sin(\omega t - \frac{2\pi}{3}) \\ \cos(\omega t + \frac{2\pi}{3}) & -\sin(\omega t + \frac{2\pi}{3}) \end{bmatrix} \begin{bmatrix} d_d \\ d_q \end{bmatrix} = \frac{2}{3} \begin{bmatrix} \cos(\omega t) & -\sin(\omega t) \\ \cos(\omega t - \frac{2\pi}{3}) & -\sin(\omega t - \frac{2\pi}{3}) \\ \cos(\omega t + \frac{2\pi}{3}) & -\sin(\omega t + \frac{2\pi}{3}) \end{bmatrix} \begin{bmatrix} D_{d0} + dm\cos(\omega_p t) \\ D_{q0} \end{bmatrix} \qquad (3\text{-}23)$$

After a simplification, equation (3-23) is written as (3-24):

$$\begin{bmatrix} d_{a\omega} \\ d_{b\omega} \\ d_{c\omega} \end{bmatrix} = \begin{bmatrix} D_{a\omega} \\ D_{b\omega} \\ D_{c\omega} \end{bmatrix} + \begin{bmatrix} \hat{d}_a \\ \hat{d}_b \\ \hat{d}_c \end{bmatrix} \qquad (3\text{-}24a)$$

$$\begin{bmatrix} \hat{d}_a \\ \hat{d}_b \\ \hat{d}_c \end{bmatrix} = \frac{1}{3} d_m \begin{bmatrix} \cos[(\omega + \omega_p)t] + \cos[(\omega - \omega_p)t] \\ \cos[(\omega + \omega_p)t - \frac{2\pi}{3}] + \cos[(\omega - \omega_p)t - \frac{2\pi}{3}] \\ \cos[(\omega + \omega_p)t + \frac{2\pi}{3}] + \cos[(\omega - \omega_p)t + \frac{2\pi}{3}] \end{bmatrix} \qquad (3\text{-}24b)$$

As can be seen in equation (3-24b), a perturbation signal with frequency ω_p in dq coordinates is modulated to $(\omega + \omega_p)$ and $(\omega - \omega_p)$ in stationary ABC coordinates. This modulation process is illustrated in Figure 3.16, where, the zero-sequence component, the da, db, and dc (60-

degree clamping SVM), and the fundamental components of da, db, and dc are compared with respect to the case with the perturbations. The power stage will respond to modulated frequency perturbations and produce small signal current and voltage on the perturbed frequencies.

3.3.2 Small Signal Model of the Power Stage

From equation (3-17), equation (3-25) can be obtained when d_a, d_b, and d_c are carry small signal perturbations: $\hat{d}_a, \hat{d}_b$ and $\hat{d}_c$.

$$\frac{d}{dt}\begin{bmatrix} i_a+\hat{i}_a \\ i_b+\hat{i}_b \\ i_c+\hat{i}_c \end{bmatrix} = -\frac{R_L}{L}\begin{bmatrix} i_a+\hat{i}_a \\ i_b+\hat{i}_b \\ i_c+\hat{i}_c \end{bmatrix} + \frac{1}{3L}\begin{bmatrix} 2 & -1 & -1 \\ -1 & -1 & -1 \\ -1 & -1 & 2 \end{bmatrix}\begin{bmatrix} v_a+\hat{v}_a \\ v_b+\hat{v}_b \\ v_c+\hat{v}_c \end{bmatrix} - \frac{(V_{dc}+\hat{v}_{dc})}{3L}\begin{bmatrix} 2 & -1 & -1 \\ -1 & -1 & -1 \\ -1 & -1 & 2 \end{bmatrix}\begin{bmatrix} d_a+\hat{d}_a \\ d_b+\hat{d}_b \\ d_c+\hat{d}_c \end{bmatrix} \tag{3-25a}$$

$$\frac{d(V_{dc}+\hat{v}_{dc})}{dt} = \frac{R_{load}}{C(R_{load}+R_c)}\begin{bmatrix} i_a+\hat{i}_a & i_b+\hat{i}_b & i_c+\hat{i}_b \end{bmatrix}\begin{bmatrix} d_a+\hat{d}_a \\ d_b+\hat{d}_b \\ d_c+\hat{d}_c \end{bmatrix} - \frac{(V_{dc}+\hat{v}_{dc})}{C(R_{load}+R_c)} \tag{3-25b}$$

In equation (3-25), (i_a, i_b, i_c), (d_a, d_b, d_c), (v_a,v_b,v_c) and V_{dc} are steady state operation points; and (i_a, i_b, i_c) and V_{dc} are solutions of the equation (3-17). (i_a, i_b, i_c), (d_a, d_b, d_c), and (v_a,v_b,v_c) are time-varying. The variables with hat are small signal perturbations. Because (i_a, i_b, i_c) and V_{dc} are the solutions of equation (3-17), equation (3-26) exists:

$$\frac{d}{dt}\begin{bmatrix} i_a \\ i_b \\ i_c \end{bmatrix} = -\frac{R_L}{L}\begin{bmatrix} i_a \\ i_b \\ i_c \end{bmatrix} + \frac{1}{3L}\begin{bmatrix} 2 & -1 & -1 \\ -1 & -1 & -1 \\ -1 & -1 & 2 \end{bmatrix}\begin{bmatrix} v_a \\ v_b \\ v_c \end{bmatrix} - \frac{V_{dc}}{3L}\begin{bmatrix} 2 & -1 & -1 \\ -1 & -1 & -1 \\ -1 & -1 & 2 \end{bmatrix}\begin{bmatrix} d_a \\ d_b \\ d_c \end{bmatrix} \tag{3-26a}$$

$$\frac{dV_{dc}}{dt} = \frac{R_{load}}{C(R_{load}+R_c)}\begin{bmatrix} i_a & i_b & i_c \end{bmatrix}\begin{bmatrix} d_a \\ d_b \\ d_c \end{bmatrix} - \frac{V_{dc}}{C(R_{load}+R_c)} = 0 \tag{3-26b}$$

In equation (3-26a), because i_a, i_b, and i_c are time-varying, the derivatives of the them do not equal to zero as in the case of time-invariant system. After subtracting equation (3-26) from (3-25), the small signal perturbation terms can be separated from the equation (3-25) as shown in equation (3-27).

$$\frac{d}{dt}\begin{bmatrix} \hat{i}_a \\ \hat{i}_b \\ \hat{i}_c \end{bmatrix} = -\frac{R_L}{L}\begin{bmatrix} \hat{i}_a \\ \hat{i}_b \\ \hat{i}_c \end{bmatrix} + \frac{1}{3L}\begin{bmatrix} 2 & -1 & -1 \\ -1 & -1 & -1 \\ -1 & -1 & 2 \end{bmatrix}\begin{bmatrix} \hat{v}_a \\ \hat{v}_b \\ \hat{v}_c \end{bmatrix} - \frac{\hat{v}_{dc}}{3L}\begin{bmatrix} 2 & -1 & -1 \\ -1 & -1 & -1 \\ -1 & -1 & 2 \end{bmatrix}\begin{bmatrix} d_a \\ d_b \\ d_c \end{bmatrix} - \frac{V_{dc}}{3L}\begin{bmatrix} 2 & -1 & -1 \\ -1 & -1 & -1 \\ -1 & -1 & 2 \end{bmatrix}\begin{bmatrix} \hat{d}_a \\ \hat{d}_b \\ \hat{d}_c \end{bmatrix} \tag{3-27a}$$

$$\frac{d\hat{v}_{dc}}{dt} = \frac{R_{load}}{C(R_{load}+R_c)}\begin{bmatrix}\hat{i}_a & \hat{i}_b & \hat{i}_b\end{bmatrix}\begin{bmatrix}d_a\\ d_b\\ d_c\end{bmatrix} + \frac{R_{load}}{C(R_{load}+R_c)}\begin{bmatrix}i_a & i_b & i_c\end{bmatrix}\begin{bmatrix}\hat{d}_a\\ \hat{d}_b\\ \hat{d}_c\end{bmatrix} - \frac{\hat{v}_{dc}}{C(R_{load}+R_c)} \quad (3\text{-}27b)$$

There is no intention to linearize the system about the operation points. The purpose of the above process is to recognize the small signal perturbation effect on the ABC coordinates. Because of the perturbation frequency modulation effect as discussed in Section 3.3.1, the perturbation frequencies of d_d and d_q on DQ coordinate and (d_a, d_b, d_c)on ABC coordinates are different. Therefore, it does not make sense to look into the transfer functions from DQ to ABC coordinates. This is illustrated in Figure 3.17. Figure 3.17 (a) shows the time domain simulation waveforms of the d channel duty cycle: dd with the perturbation and the state variables: the phase A current and output dc bus voltage. Figure 3.17 (b) shows the frequency spectrum of these waveforms. As shown in these Figures, the frequency spectrum of ia and dd are differed by ω_p. Therefore, the transfer function from dd to ia has no meaning. However, the transfer functions on DQ coordinates can still be obtained, for example transfer function from dd and dq to id and iq. This is because the dual frequency perturbation ($\omega+\omega_p$) and ($\omega-\omega_p$) on ABC coordinate are transformed into a single perturbation frequency ω_p after the ABC to DQ transformation is performed

Figure 3.17 also shows the frequency spectrum of the dc bus voltage, which has the same frequency peak as the dd channel perturbation. This is because even though the small signal ($\hat{i}_a, \hat{i}_b, \hat{i}_c$) and ($\hat{d}_a, \hat{d}_b, \hat{d}_c$) in equation (3-27b) have dual frequency perturbation, the product with (d_a, d_b, d_c), and (i_a, i_b, i_c) in equation (3-27b) shows the original frequency.

3.3.3 Small Signal Perturbation Propagated onto DQ Coordinates

The small signal perturbations in the three-phase currents are transformed through the following transformation into DQ coordinates:

$$\begin{bmatrix}i_d\\ i_q\\ i_0\end{bmatrix} = \sqrt{\frac{2}{3}}\begin{bmatrix}\cos(\omega t) & \cos(\omega t-\frac{2\pi}{3}) & \cos(\omega t+\frac{2\pi}{3})\\ -\sin(\omega t) & -\sin(\omega t-\frac{2\pi}{3}) & -\sin(\omega t+\frac{2\pi}{3})\\ \sqrt{\frac{1}{2}} & \sqrt{\frac{1}{2}} & \sqrt{\frac{1}{2}}\end{bmatrix}\begin{bmatrix}i_a+\hat{i}_a\\ i_b+\hat{i}_c\\ i_c+\hat{i}_c\end{bmatrix} = \begin{bmatrix}I_d\\ I_q\\ i_0\end{bmatrix} + \begin{bmatrix}\hat{i}_d\\ \hat{i}_q\\ \hat{i}_0\end{bmatrix} \quad (3\text{-}28)$$

Assuming the perturbed components in i_a, i_b, and i_c at the modulated frequencies are:

$$\begin{cases} \hat{i}_a = I_{\omega+\omega_p}\cos[(\omega+\omega_p)t+\varphi]+I_{\omega-\omega_p}\cos[(\omega-\omega_p)t+\varphi'] \\ \hat{i}_b = I_{\omega+\omega_p}\cos[(\omega+\omega_p)t+\varphi-\frac{2\pi}{3}]+I_{\omega-\omega_p}\cos[(\omega-\omega_p)t+\varphi'-\frac{2\pi}{3}] \\ \hat{i}_c = I_{\omega+\omega_p}\cos[(\omega+\omega_p)t+\varphi+\frac{2\pi}{3}]+I_{\omega-\omega_p}\cos[(\omega-\omega_p)t+\varphi'+\frac{2\pi}{3}] \end{cases} \quad (3\text{-}29)$$

In equation (3-29), $I_{\omega+\omega_p}, I_{\omega-\omega_p}$, ϕ, and ϕ' are the magnitude and the phase angle of the small signal current at the modulated frequencies. By inserting (3-29) into (3-28), equation (3-30) can be obtained after a few steps of simplification:

$$\hat{i}_d = \frac{1}{2}\sqrt{\frac{2}{3}}\frac{d_m V_{c0}}{\sqrt{R_L{}^2+(\omega+\omega_p)^2L^2}}\cos(\omega_p t+\varphi)+\frac{1}{2}\sqrt{\frac{2}{3}}\frac{d_m V_{c0}}{\sqrt{R_L{}^2+(\omega-\omega_p)^2L^2}}\cos(\omega_p t-\varphi') \quad (3\text{-}30a)$$

$$\hat{i}_q = -\frac{1}{2}\sqrt{\frac{2}{3}}\frac{d_m V_{c0}}{\sqrt{R_L{}^2+(\omega+\omega_p)^2L^2}}\sin(\omega_p t+\varphi)+\frac{1}{2}\sqrt{\frac{2}{3}}\frac{d_m V_{c0}}{\sqrt{R_L{}^2+(\omega-\omega_p)^2L^2}}\sin(\omega_p t-\varphi') \quad (3\text{-}30b)$$

Equation (3-30) shows that the small signal three-phase currents with multiple frequency spectra are transformed back into the perturbation frequency again. The detailed derivation process is shown in the appendix. The abc/dq transformation does the reversed frequency modulation effect of the SVM.

The above process reveals the small signal perturbation and propagation process in three-phase systems with a SVM control. This process is similar to the hardware measurement method, in which the perturbation is injected into the system from dd or dq, and the DQ channel variables id and iq are measured. Therefore, with the PEBB-based modeling approach, the power stage is modeled on the ABC coordinates, the system small signal transfer functions on DQ coordinates still can be obtained.

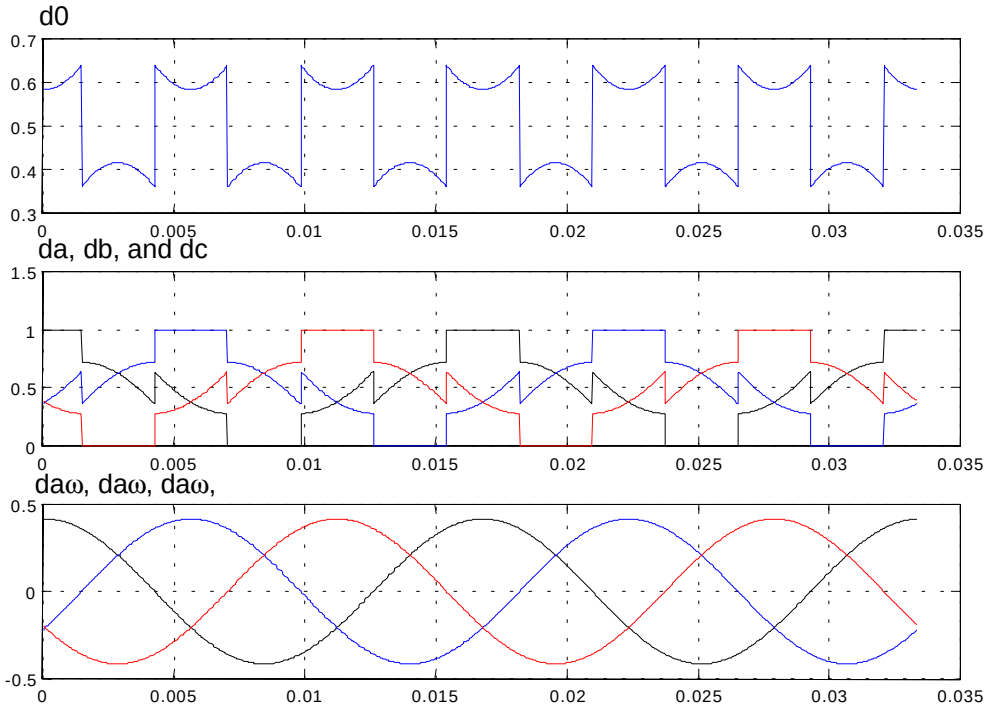

(a)

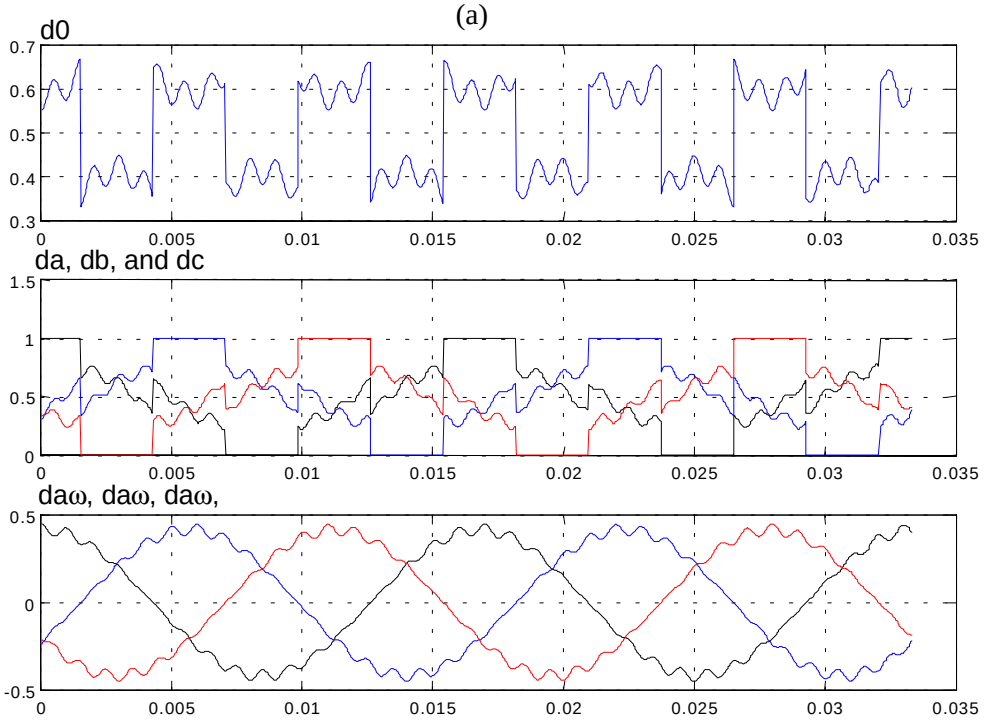

(b)

Figure 3.16 The waveforms of the 60-degree clamping SVM, (a) without small signal perturbation, (b) with 1 kHz small signal perturbation on d_d

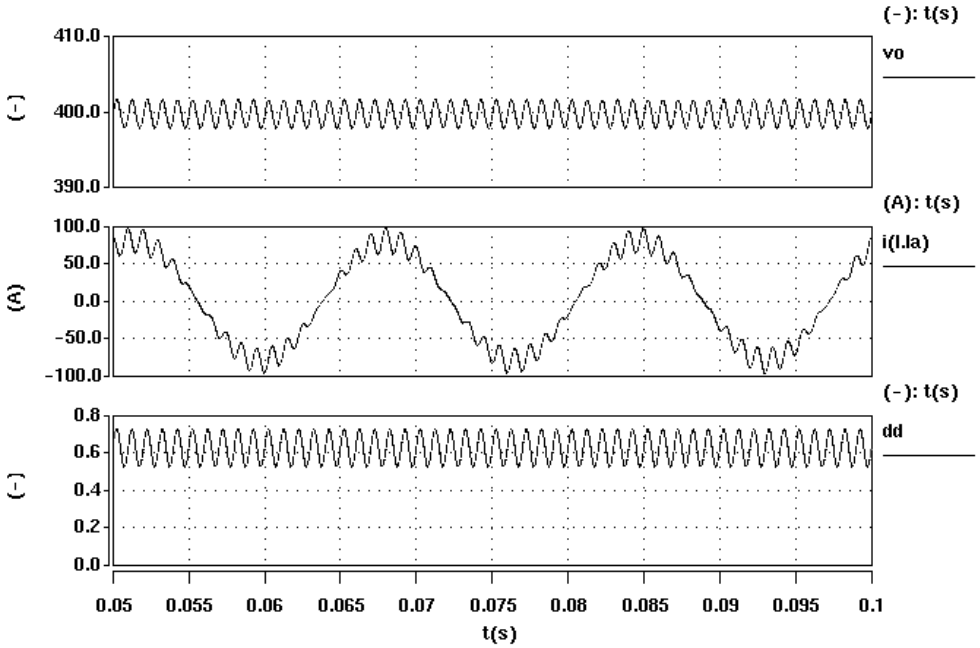

(a)

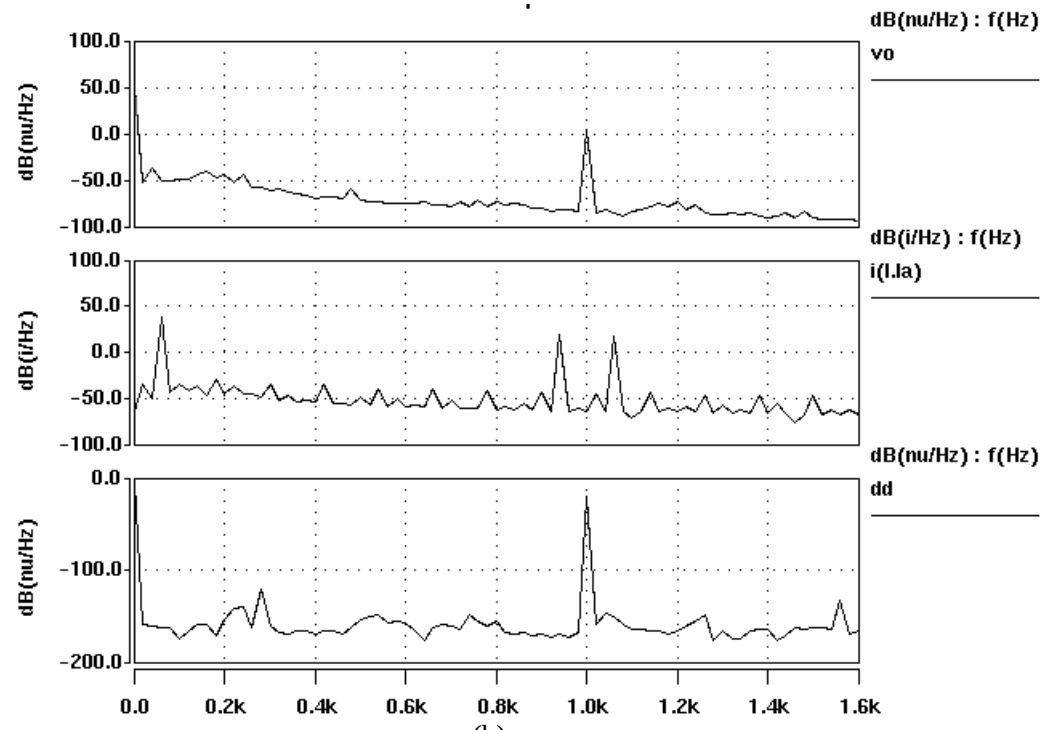

(b)

Figure 3.17 (a) Time domain simulation waveform of Vo, Ia, and dd, (b) Corresponding frequency spectrum

3.3.4 Small Signal Analysis Based on Average Circuit Model

Using the average model, the small signal analysis is performed. The Saber has a built-in function in "Analog System Synthesis" component library, which provides a component similar to the Impedance/Gain-Phase Analyzer. It can generate the perturbation signals by sweeping a user-defined frequency range. The DQ channel components can be measured by connecting the measurement channels to them. The measurement channel has a filter option in order to pick up the perturbation frequency.

Figure 3.18 and 3.19 show the Bode plot of the open loop transfer functions of $\hat{i}_d / \hat{d}_d$ and $\hat{i}_q / \hat{d}_d$ in comparison with the curves obtained with dq model. The two curves match very well each other. The discrepancy at high frequency is caused by the filtering effect.

Figure 3.20 shows the Bode plots of the output impedance of the rectifier obtained from two models. The output impedance is attenuated by the voltage loop gain at low frequency range. The capacitor branch impedance will dominate at high frequency range. The phase of the impedance changes from inductive 90-degree to capacitive 90-degree and comes back to zero degree related to the ESR of the output capacitor.

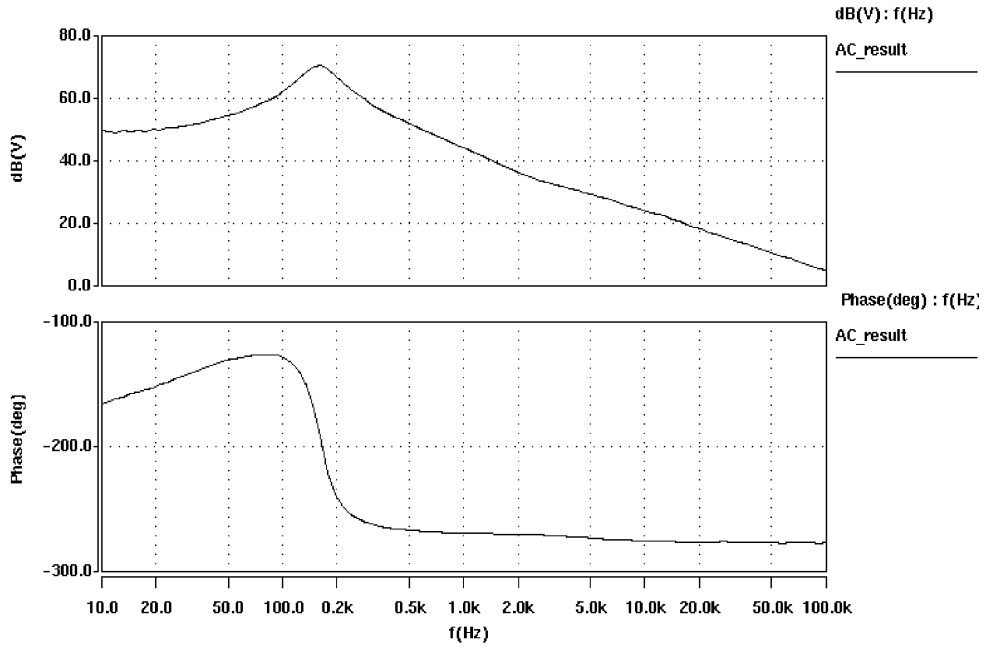

(a)

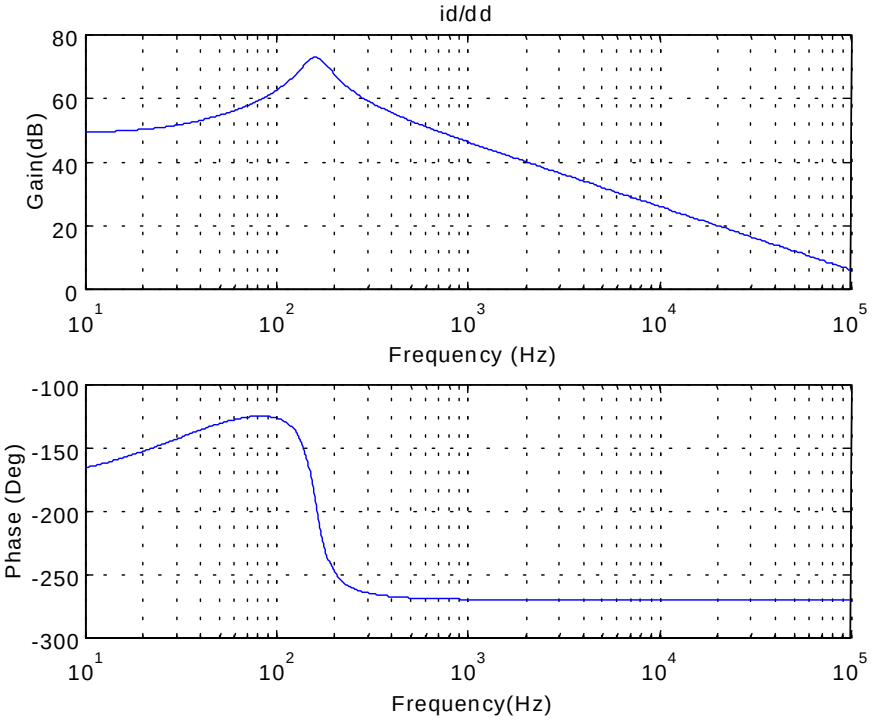

(b)

Figure 3.18 Comparison of the open loop transfer function from dd to id (a) with the average model (b) with DQ model

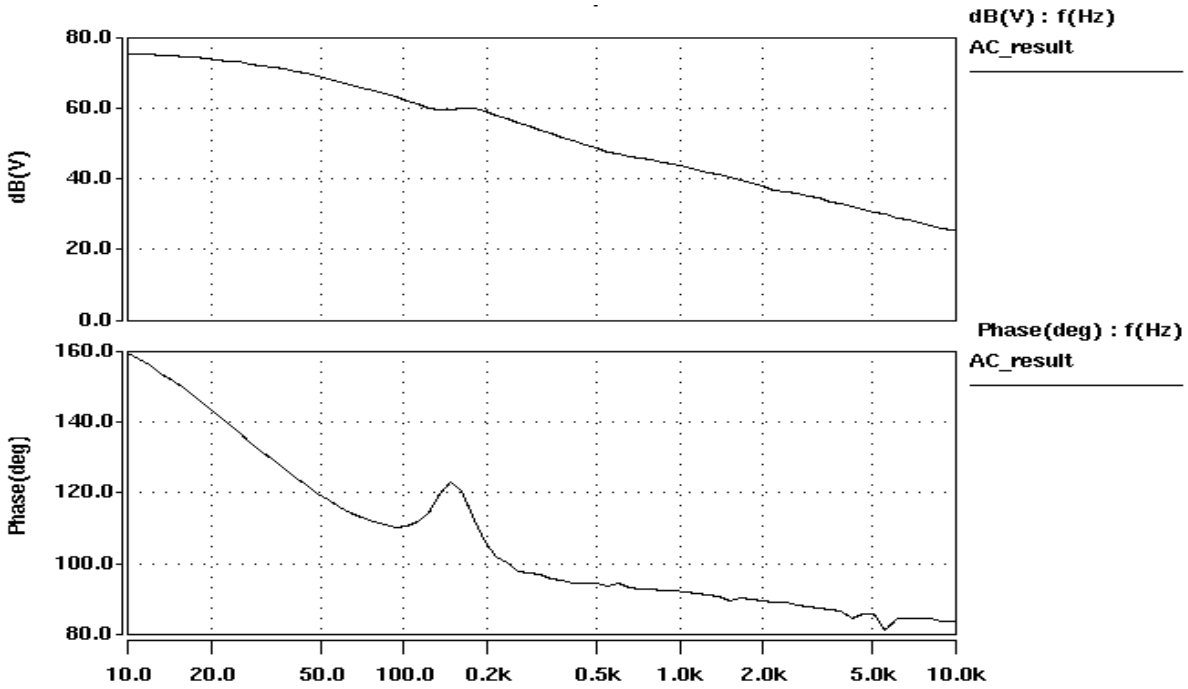

(a)

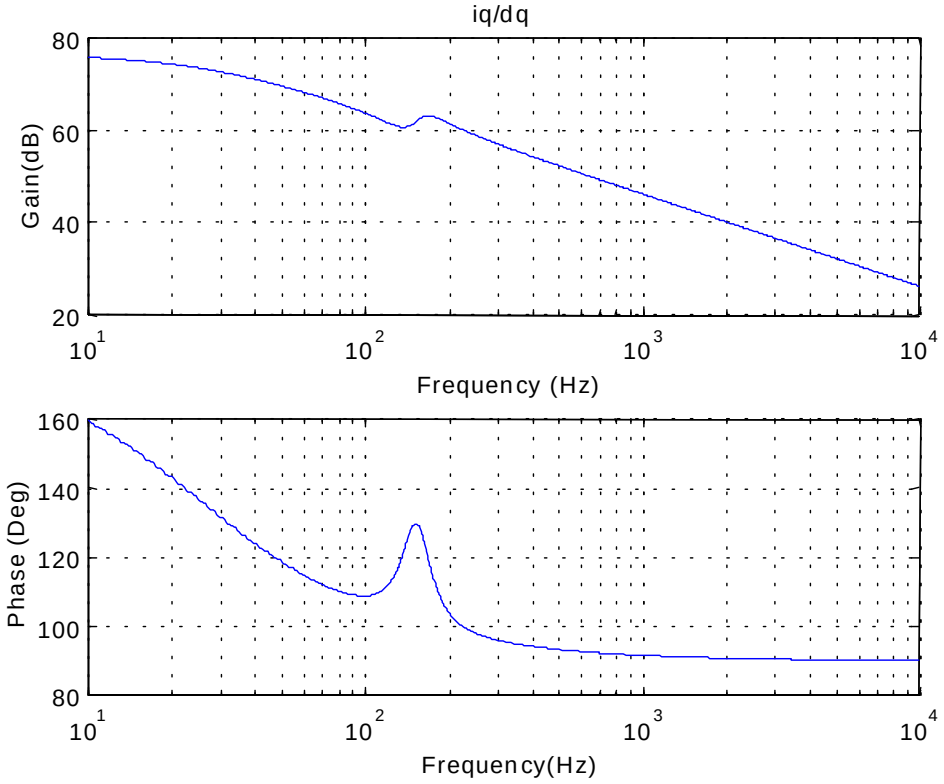

(b)

Figure 3.19 Comparison of the open loop transfer function from dq to iq (a) with the average model (b) with the DQ model

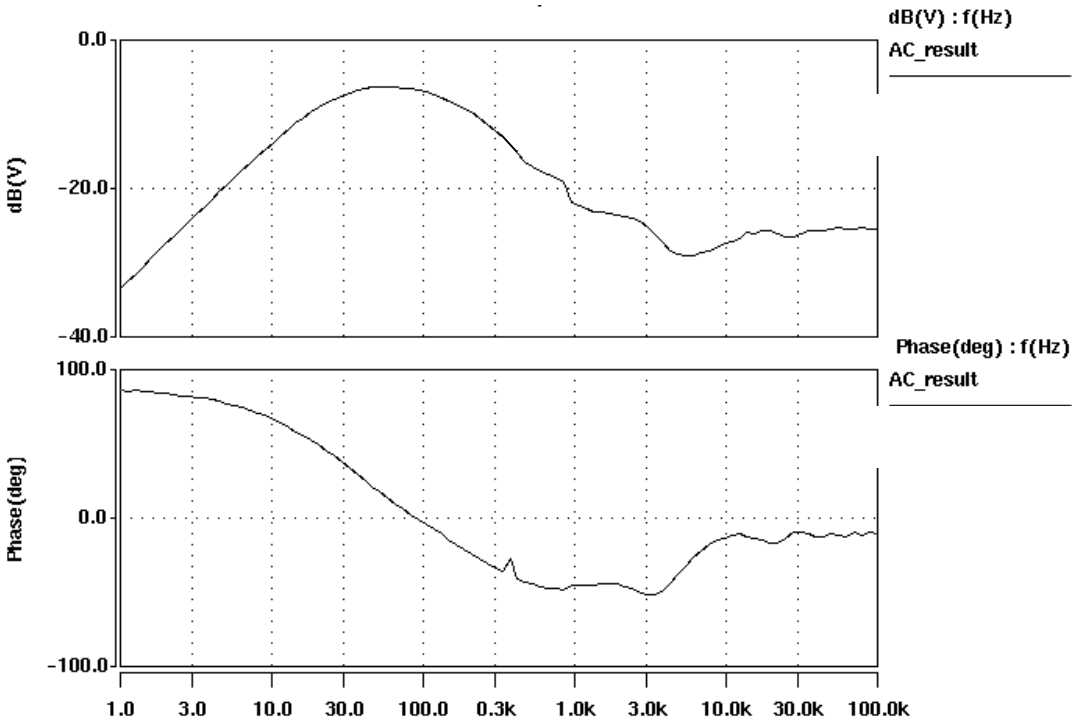

(a)

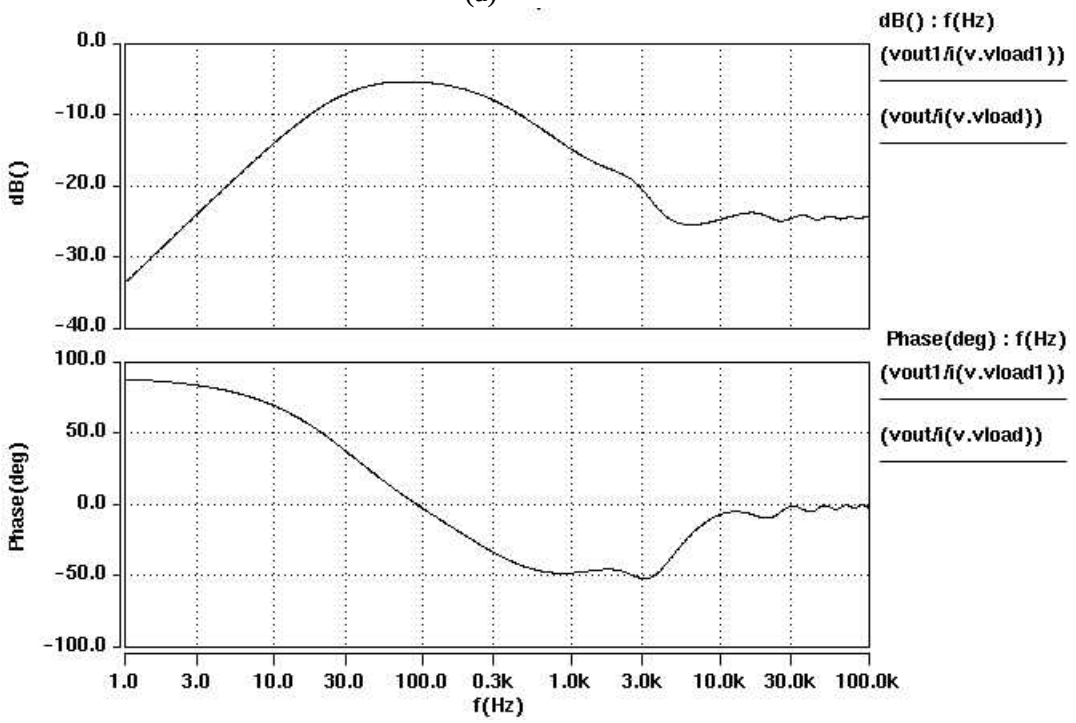

(b)

Figure 3.20 Comparison of the output impedance of the front-end rectifier, (a) with the average model (b) with the DQ model